

SMARTLAGOON

DELIVERABLE 3.1

Complete SWAT+ model setup for Mar Menor



This project has received funding from the European Union's Horizon 2020 research and innovation programme under grant agreement No 101017861.



Innovative modelling approaches for predicting Socio-environmental evolution in highly anthropized coastal LAGOONS

Deliverable 3.1

Deliverable No.:	3.1
Project Acronym:	SMARTLAGOON
Full Title:	Innovative modelling approaches for predicting Socio-environmental evolution in highly anthropized coastal LAGOONS
Grant Agreement No.:	101017861
Workpackage/Measure No.:	WP3
Workpackage/ Measure Title:	Innovative modelling of environmental processes
Responsible Author(s):	Javier Senent-Aparicio (UCAM)
Responsible Co-Author(s):	Inmaculada Jiménez-Navarro (UCAM) Adrián López-Ballesteros (UCAM) Don Pierson (UU) Dennis Trolle (WIT)
Date:	30/06/2022
Status:	
Dissemination level:	Public

HISTORY OF CHANGES		
Date	Content	Author(s)

The content of this deliverable represents the views of the authors only and sole responsibility; it cannot be considered to reflect the views of the European Commission or any other body of the European Union. The European Commission and the Agency do not accept any responsibility for use that may be made of the information it contains.

Abstract

SMARTLAGOON Project benefits from the support of the Horizon 2020 programme of the European Union within the framework of an Innovation Action. To ensure the development of their activities to achieve the expected results the eight organizations members of the consortium will release some deliverables during the timeline of the project (48 months in total). These deliverables are numbered and depend on each Work Package.

The present deliverable D3.1 is the first deliverable of the Work-Package 3. The focus of this Work-Package is to develop innovative modelling of the Mar Menor environmental processes in a holistic way. This implies taking into account the water balance of the watershed, the ecological, physical and chemical dynamics of the water body; and its connections with the Mediterranean Sea. This will be achieved by combining physical and ecological models. The first task for this is the development of physically based catchment models, applying the semi-distributed SWAT+ model to the catchment of the Mar Menor and Lake Erken for simulation of hydrology and estimates of sediment and nutrient inputs. Hydrological modeling in both the Campo de Cartagena basin of Mar Menor and in the Erken Lake pilot basin, have been carried out with both the SWAT and the SWAT+ model (latest version released is dated May 6, 2022). Given the recent release of SWAT+ this document presents all the modeling carried out to date and, of course, will be continuously updated as new SWAT+ model capabilities are tested, and new observation data are obtained from the instrumentation installed for this purpose within the framework of the SMARTLAGOON project.

In this deliverable we explain the development of these two physical models with SWAT and SWAT+ step by step. First, we offer a description of both study areas. Next we explain what input data is required to develop the SWAT models and how we obtained it for both basins. Then, the process of creation of hydrologic response units in SWAT is discussed, followed by the methods used to calibrate and validate the models. Finally, we describe the calibrations that have been carried out, providing the results obtained, and present a brief description of the hydrological cycle of the Mar Menor and Lake Erken basin thanks to the SWAT simulation.

The hydrological cycle of the Mar Menor, characterized by its high degree of anthropization and the absence of specific flow information, has been calibrated using measured evapotranspiration data from remote sensing. The Lake Erken basin, for which there is a historical record of water discharge, has been calibrated with these data and satellite-derived snow water equivalent. After calibration, the two models show good performance in simulating components of the hydrological cycle that could be compared to the real measurements. An overview of the hydrological balance taking place in both basins has been obtained.

TABLE OF CONTENT

Abstract	3
1. Introduction	5
1.1 Motivation	5
1.2 Goals	6
1.3 Interest in the results	6
1.4 Methodology	7
1.5 Study areas	8
1.5.1 Lake Erken.....	8
1.5.2 Mar Menor.....	10
2. Required input data	12
2.1 Spatial data	12
2.1.1 Lake Erken.....	12
2.1.2 Mar Menor.....	13
2.2 Climatic data	14
2.3 Calibration data	15
3. Development of the models	16
3.1 Sub-basin delimitation	16
3.2 Sensitivity analysis, calibration and validation	16
3.3 Evaluation of the models	18
4. Results	19
4.1 SWAT12 Lake Erken model	19
4.1.1 Warm-up, calibration and validation periods.....	19
4.1.2 Streamflow calibration and validation.....	20
4.1.3 Water balance of the Lake Erken watershed.....	21
4.2 SWAT+ Lake Erken model	22
4.2.1 Warm-up, calibration and validation periods.....	22
4.2.2 Streamflow calibration and validation.....	23
4.2.3 Snowpack calibration and validation.....	24
4.2.4 Sediment and nutrients future calibration.....	26
4.2.5 Water balance of the Mar Menor watershed.....	27
4.3 SWAT12 Mar Menor model	28
4.3.1 Warm-up, calibration and validation periods.....	28
4.3.2 Evapotranspiration calibration and validation.....	28
4.3.3 Water balance of the Mar Menor watershed.....	30
4.4 SWAT+ Mar Menor model	30
4.4.1 Warm-up, calibration and validation periods.....	30
4.4.2 Evapotranspiration calibration and validation.....	31
4.4.3 Water balance of the Mar Menor watershed.....	32
5. Conclusion	33
Appendix I	34
Appendix I.I: Description of the SWAT and SWAT+ model	35
Appendix II: Bibliography	42

1. Introduction

1.1 Motivation

This document is the first deliverable of the Work-Package 3 (WP3) of the SMARTLAGOON project, led by the UCAM. The focus of this Work-Package is to develop innovative modelling of the Mar Menor environmental processes in a holistic way. This implies taking into account the water balance of the watershed, the ecological, physical and chemical dynamics of the water body; and its connections with the Mediterranean Sea. This will be achieved by combining physical and ecological models. The first task for this is the development of physically based catchment models, applying the semi-distributed SWAT+ model to the catchment of the Mar Menor and Lake Erken for simulation of hydrology and estimates of sediment and nutrient inputs.

Hydrological models have been used for decades to assist in the management and planning of water resources throughout the world. These models simulate the components of the hydrological balance of a watershed, such as the streamflow, the evapotranspiration, the percolation, or even the snowpack. The hydrological models help to estimate the water resources of an area and to predict how changes on the land uses or the climate will affect these resources. More importantly, hydrological models have the ability to be adapted to simulate the climatic, geographic and human conditions of particular catchments, if sufficient data are available. This allows for local management of water resources, which is indispensable for the implementation of appropriate measures (Brekke *et al.*, 2004). To develop and ensure that a hydrological model is acceptable, real data is needed to perform model calibration and validation.

The Campo de Cartagena hydrological basin of the Mar Menor, is highly anthropized (Jiménez-Navarro, 2020). This, together with the limited real data available to calibrate the basin model, makes the development of a physical hydrological model challenging. In addition, its lagoon presents a complex and delicate ecosystem, which will require the development of a subsequent ecological model, and, finally, the integration of both, in order to obtain useful predictions of the Mar Menor water quality. To achieve this integration, we need to understand the connection between the watershed and the lagoon and the cause-effect phenomena that occur in them. The first step is to develop an accurate model of the Campo de Cartagena to know how much water enters the lagoon from the basin and what materials it carries with it.

Due to the aforementioned complications in the Mar Menor basin, we used Lake Erken (Sweden) as a site to test and develop the models that will be used at Mar Menor. Lake Erken is one of the very few lakes in Northern Europe that has a long history of monitoring, including both manual and high-frequency automatic measurements of lake and stream stations. This monitoring is carried out by the Uppsala University Department of Ecology and Genetics. The Lake Erken watershed is also very predictable since it does not have a high level of anthropization. These data provide a strong foundation for model development.

1.2 Goals

The aim of this deliverable is to report on the progress made in the development of the physically based SWAT+ model of the Mar Menor watershed. And in order to obtain this model, a SWAT model of the Lake Erken basin has been developed, which will also be described in this deliverable. In the same way, the steps that have been followed and how the difficulties encountered in the development of this project have been solved will be shown.

The specific goals in this study are:

- Obtain sufficient input data for SWAT modelling of the Lake Erken and Mar Menor basins: spatial data and climatic data.
- Obtain sufficient measured data to be able to calibrate and validate the models. Depending on the basin and the availability of real data, direct or automatic measurements of flows, nutrients or sediments (Lake Erken) or satellite remote sensing products such as evapotranspiration (Mar Menor) will be used.
- Modelling the hydrology of both Lake Erken and Mar Menor basins, in an appropriate way to meet the conditions of each basin, including snow processes in the Lake Erken and agricultural management and crop development in the Mar Menor for a better quantification of water resources.
- Calibrate and validate both models to ensure their usefulness and the reliability of their output data. This data will be used in the future to integrate both SWAT models with ecological models of Lake Erken and the Mar Menor lagoon.

1.3 Interest in results

The availability of a functional model of the catchment areas of Lake Erken and the Mar Menor will allow, firstly, a better understanding of these watersheds and of the hydrological processes occurring within them. A deeper understanding of these processes is essential, especially in the case of the Mar Menor, due to its complexity and high anthropization.

The results obtained will make it possible to reduce the uncertainty associated with other calculations related to the ecological status of the Mar Menor derived from its relationship with the catchment areas and hydrologic response. The modelling of the transport of sediment and nutrients (nitrates and phosphates) entering the lagoon via the seasonal rivers has a special relevance in this project, since this is the main cause of contamination of the Mar Menor (Aguilar Escribano *et al.*, 2016). This model will make it possible to predict and analyze the effects of different agricultural practices aimed at reducing the input of sediments and nutrients into the Mar Menor lagoon. This will enable the most efficient measures to be taken to guarantee the environmental sustainability of the Mar Menor environment.

On the other hand, developing a model of the Lake Erken basin and integrating it with a model of its lake will allow us to extensively test and establish the methodology for coupled model simulations that provide more holistic and accurate simulations of lakes and their draining basins.

1.4 Methodology

The Soil and Water Assessment Tool (SWAT) (Arnold *et al.*, 2012) is a software that allows the development of hydrological watershed models. It was used to achieve the above objectives. It has been successfully used in a range of scenarios with different climatic conditions, land management practices, and temporal and spatial scales. During the last 20 years, SWAT has been implemented periodically to meet the diverse requirements of the scientific community around the world. However, the current framework has reached the limit of its potential development, and a new most recent version, SWAT+ has been developed. SWAT+, improves runoff routing capabilities while preserving the model's computational efficiency and ease of use (Bieger *et al.*, 2017).

For the development of this project, the SWAT model was chosen for several reasons: (a) close relationship between the reasons for developing the model and the objectives set out in this research; (b) SWAT is an open access program; (c) and it has been successfully applied in areas with diverse spatial and environmental conditions (Gassman *et al.*, 2007). While the older version of SWAT (hereafter referred to as SWAT12) is less flexible, it is also more useful in many instances, as it has been tested much more. For this reason, a total of four models have been developed: an Erken Lake SWAT12 model, an Erken Lake SWAT+ model, a Campo de Cartagena SWAT12 model and a Campo de Cartagena SWAT+ model.

A description of the SWAT12 and SWAT+ model can be found in appendix I.

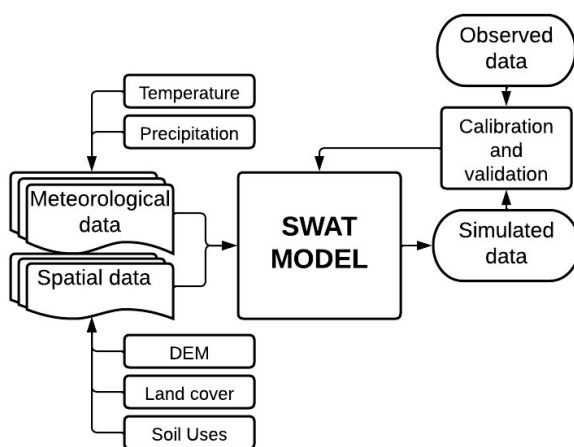


Figure 1. Flowchart of the process for develop a SWAT model.

The first step was to obtain all the input data required to develop both the Erken and Mar Menor watershed SWAT models. This required data that can be divided in spatial data and meteorological data. The spatial data needed is a digital elevation map (DEM), a land cover map, and a soil map. With this information SWAT recreates the geography of the watershed. The meteorological input data required is monthly or daily precipitation and temperature. The SWAT model can also use solar radiation, wind speed and humidity data. if the Penman-Monteith method is used to determine potential evapotranspiration rather than the Hargreaves method that requires only the precipitation and temperature data (Hargreaves, 1994). According to Oudin *et al.*, 2005, hydrological models that employ parsimonious temperature-based methods perform similarly to models that use more data-demanding methods.

Next step is the calibration and validation of the models. In order to perform the calibration properly, sensitivity analyses were first performed to determine which parameters are most important in each model. To calibrate SWAT models observed data is required. Usually, streamflow data is used, but other type of data can also be used. To calibrate the Erken model streamflow data was used along with the snow water equivalent (SWE), due the importance of the snow parameters in the hydrological cycle of basins towards the poles. On the other hand, to calibrate the Mar Menor model there wasn't enough observed streamflow data since most of the streams are ephemeral. This complicates the calibration, and for this reason, we used actual evapotranspiration data (AET) from remote sensing data to calibrate the model. Finally, at least in Lake Erken, where we have sediment and nutrient data, it is intended to calibrate with this information, since it will be the input data for the WET model in the future.

1.5 Study areas

In this section we will describe the two areas to be modelled: Lake Erken and the Mar Menor. We will describe their drainage basins and water bodies, the climate and geography of the site and its human context.

1.5.1 Lake Erken

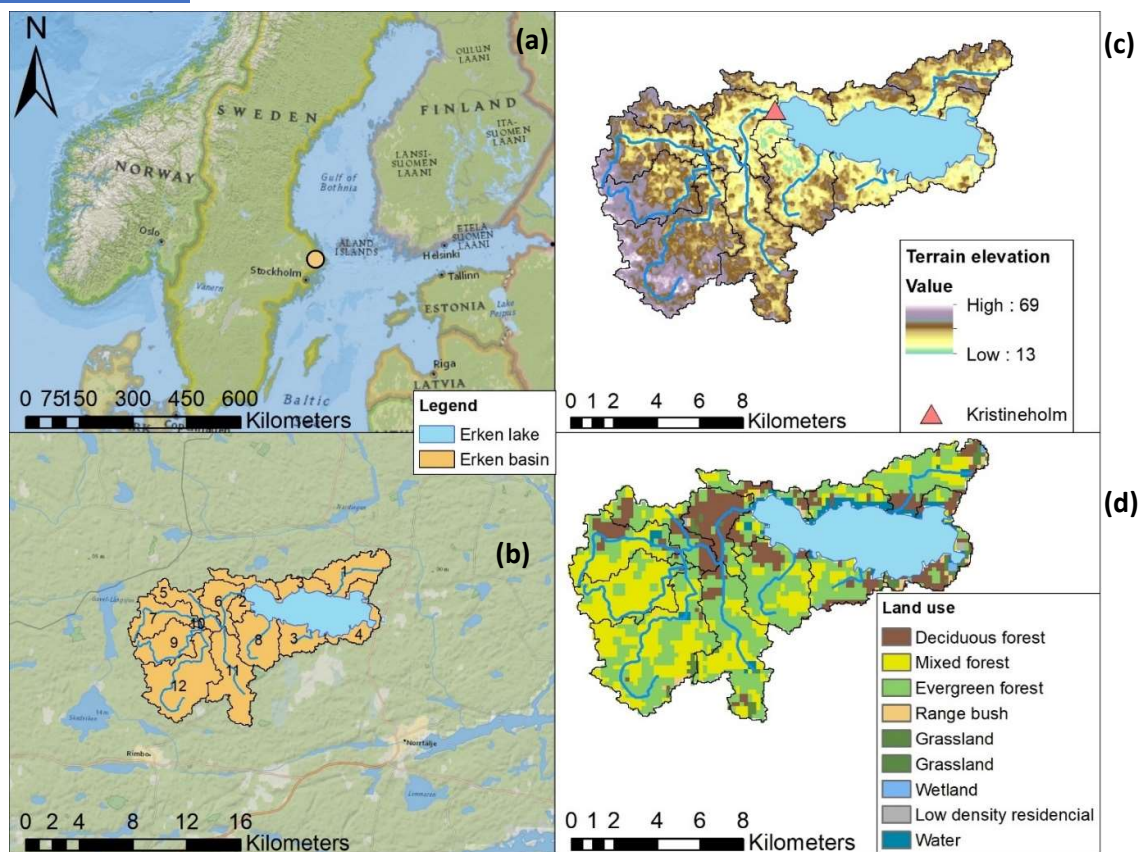


Figure 2. Map of the study area in Sweden: (a) localization of Lake Erken and its basin in the Scandinavian Peninsula; (b) watershed of the Lake Erken divided in sub-basins by SWAT; (c) digital elevation map of the Lake Erken basin and location of Kristineholm and the weather station; (d) land uses in the Lake Erken basin.

Lake Erken can be described as a moderately eutrophic lake with an intermediate level of productivity. Its surface is usually ice-covered during winter, whereas during the summer, the water is stratified. Both of these phenomena have been extensively studied by the Uppsala University and many guest researchers who have used the lake in their studies. It is a shallow lake, the mean depth is around 9 m, and the deepest point is 21 m underwater. Its surface area is approximately 24 km². The lake has a residence time of 7.4 years. Lake Erken is located in the eastern part of Sweden (59°50'37"N, 18°35'38"E) at an altitude of 10 m above sea level (Figure 2).

The Erken basin is oriented toward the east and does not present significant slopes (Figure 2(c)). It is a relatively small drainage basin (135km²) that is covered by forest, with small areas of agricultural grazing and pasture (Malmaeus & Håkanson, 2004). In the basin, there are exclusive areas of both deciduous forest and evergreen forest although, in most of the basin, both types of vegetation share the space, forming a mixed forest that dominates the watershed (Figure 2(d)). The main large water inflow point to the lake is the Kristineholm (Figure 2(c)). This input is where the water discharge for calibration and validation is measured.

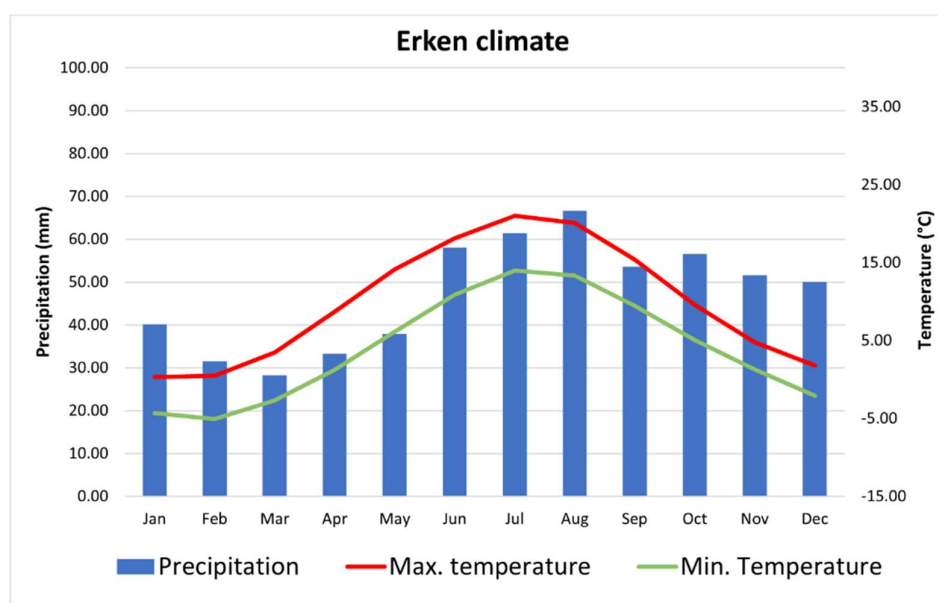


Figure 3. Average monthly temperature and precipitation in the Lake Erken basin.

In the south-central area of Sweden where Erken is located, the climate is humid and continental, with a warm summer and a moderate winter (Figure 3)—despite the country’s high latitude. The length of daylight varies from 18 h in June to 6 h in December. According to the historical data obtained from the Erken Laboratory (represented as “weather station” in figure 2(c)) for 1990–2021, in the Erken basin the warmer month was July with an average temperature of 17.5 °C. The coldest month is February with -2.32°C average temperature. Precipitation does not change much during the year but is slightly higher during summer (June, July and August); the annual average is 519 mm. Precipitation in the form of snowfall occurs between December and March, the basin is covered by snow for 75 to 100 days a year.

1.5.2 Mar Menor

The Mar Menor is a hypersaline coastal lagoon with an immense socio-economic and ecological value and a clear case of a severely anthropized hydro-ecosystem in southeastern Spain (Velasco *et al.*, 2018). It has a surface area of 135 km² covering a coastline of 73 km and contains five volcanic islands. The Mar Menor is considered a shallow lagoon, with an average depth of 4.4 m, being the maximum depth around 7 m. La Manga, a 22 km long sandy coastal barrier, isolates the lagoon from the Mediterranean Sea and is intersected by three inlets (Las Encañizadas, El Estacio y Marchamalo), facilitating exchanges of waters between the Mediterranean Sea and the lagoon (Figure 4). The most important water exchange takes place through the Estacio channel.

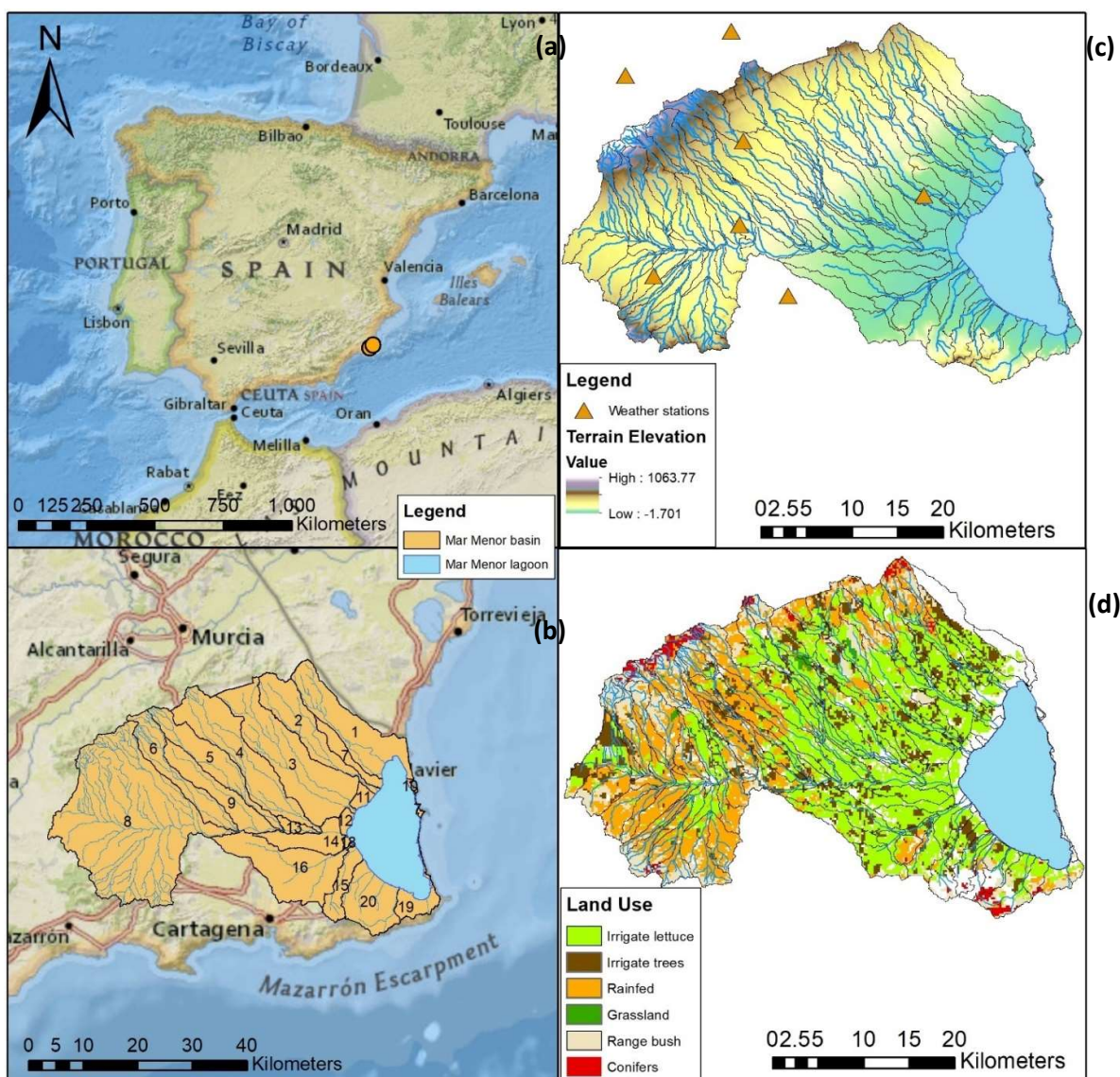


Figure 4. Map of the study area in Spain: (a) localization of Mar Menor and its basin in the Iberian Peninsula; (b) watershed of the Mar Menor divided in sub-basins by SWAT; (c) digital elevation map of the Mar Menor basin and location of the weather station; (d) land uses in the Campo de Cartagena.

The catchment area of the Mar Menor is known as the hydrological basin of Campo de Cartagena. Water enters the lagoon through several seasonal ephemeral riverbeds. The most important is the Albuji3n wadi, which is active throughout the year with a very low streamflow. Most of the other wadis only deliver water flow after significant rainfall events. The lagoon's economic, social, and urban evolution during the last half-century has had a variety of effects on the physical and natural environment, making the Mar Menor a special-protected area. Due to the high level of anthropization, the Mar Menor is in a deteriorated state. This is a common problem in coastal lagoons (Le Moal *et al.*, 2019). Two main anthropic activities occur on this basin: agriculture and tourism. Most of the watershed area is used as arable land, especially for irrigated agriculture (vegetable such as lettuce), although part of it is also used for citrus, almond and olive cultivation (Figure 4(d)). Water scarcity in the region has resulted in the use of drip irrigation and the need to make efficient use of water (Senent-Aparicio *et al.*, 2015). Irrigated agriculture in Campo de Cartagena saw a pronounced increase at the end of the 20th century, which led to a considerable increase in fertilizer inputs to the basin. At present, the Campo de Cartagena is one of the main horticultural producers in Europe (Velasco *et al.*, 2006). The Mar Menor and its surroundings have been a popular tourist destination in the region of Murcia since the 1960s, when its urbanization began (Morales Yago, 2013). Although the climatological and environmental conditions of La Manga del Mar Menor are ideal for supporting tourism throughout the year, the occupancy rate soars during the summer period (Esteve Selma *et al.*, 2016).

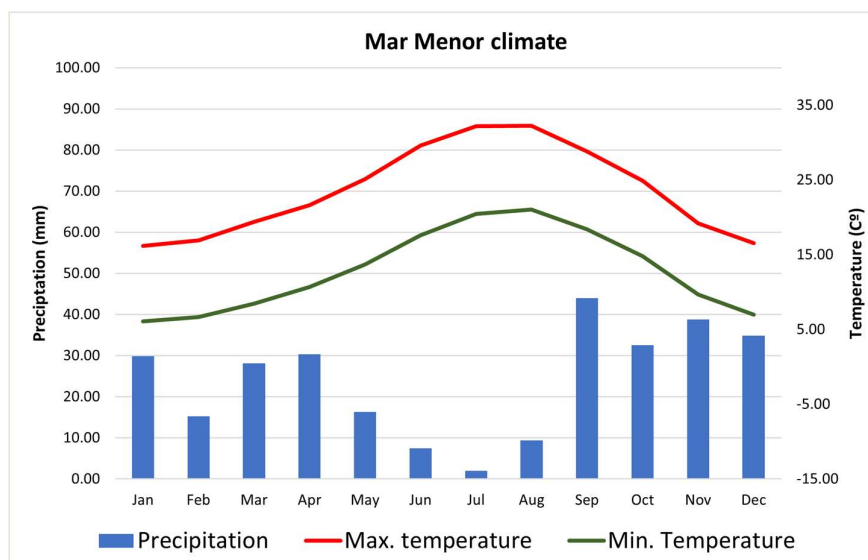


Figure 5. Average monthly temperature and precipitation in the Mar Menor basin.

In Murcia, the climate is Mediterranean and semi-arid, since it receives precipitation below the potential evapotranspiration. Summers are dry and hot and winters are mild (Figure 5). According to the weather data used in this study, this basin is one of the most arid of the Mediterranean area, the warmer month was August with an average temperature of 26.6°C. The coldest month is January with 11.1°C average temperature. Annual precipitation ranges from 166 mm to 469 mm, where

average precipitation is less than 300 mm per year. The precipitation is unevenly distributed occurring seasonally, mainly in autumn and spring, in punctual and torrential events.

2. Required input data

For the simulation of hydrologic processes, the SWAT model divides the watershed into sub-watersheds based on the drainage network and topography. SWAT also considers the spatial heterogeneity of a watershed by dividing the subwatersheds into multiple hydrologic response units (HRUs). Water dynamics are represented by fluctuations in the HRUs in both the SWAT12 and SWAT+ models. Each HRU is a unique combination of land-use, slope, soil, and management activities, and are calculated using a geographic information system (GIS) interface. Using this GIS interface, in both models, the modelled basin is divided into various sub-basins, which are further sub-divided into HRUs (Mohammed *et al.*, 2018).

This chapter describes the information necessary for the HRUs creation and the implementation of the model: spatial data (a digital elevation map (DEM), a land cover map and a soil map) and climatological information (daily precipitation and temperature data).

A description of the collected information required by the model as input data is discussed below.

2.1 Spatial data

Land use has a great influence on the hydrological properties of watersheds, so it is necessary to consider it during hydrological modeling. Soil maps were used to characterize each soil type based on information on soil texture, hydraulic conductivity and available water content, among others. Land use is one of the most important factors controlling events such as runoff, evapotranspiration, sediment deposition, and soil erosion.

The development of a hydrological model with SWAT requires this specific geographical information about the area of interest. The data required include a digital elevation map (DEM), a land cover map, and a soil map. Also, the slopes on the basin should be defined in categories. These maps will be connected by a geographic information system (GIS) interface: QGIS, using the plugins QSWAT and QSWAT+. With this information SWAT will develop a first model of the watershed based in HRUs.

2.1.1 Lake Erken

For the Lake Erken, the DEM was obtained from the Shuttle Radar Topography Mission (SRTM). The SRTM uses a single-pass space-borne interferometric SAR system, which operates in both the C-band (5.6-cm) and the X-band (3-cm) frequencies to collect data about the earth's surface elevation (Farr & Kobrick, 2000). The DEM of the Lake Erken is represented in Figure 2(c).

The land cover map of the Lake Erken basin was obtained from Glob Cover 2015, which provides a 300-m resolution (Arino *et al.*, 2010). This was used for the SWAT+ model of the Erken Lake. The different land uses of the Erken basin are represented in Figure 2(d).

For the SWAT12 model of the Erken Lake we used the CORINE Land Cover (CLC) dataset, which was initiated in 1985 (reference year 1990), provided by Copernicus Land Monitoring Service (CLMS). Updates have been produced in 2000, 2006, 2012, and 2018. It consists of an inventory of 44 land cover classes, and comes in a raster resolution of 100 m.

The soil data were gathered from the Food and Agriculture Organization of the United Nations' Harmonized World Soil Date. This collection contains information for 16,000 map units with two soil layers, namely 0–30 and 30–100 cm deep (Nachtergaele *et al.*, 2010).

Three slope categories (0-2%, 2-8% and > 8%) were defined and a threshold level of 10% was set to simplify model processing and eliminate slopes, soils and minor land uses used for each subwatershed.

The physical characteristics and land use of the Lake Erken watershed are discussed in section 1.5.1.

2.1.2 Mar Menor

Streams and the drainage basin of the Mar Menor were derived based on a DEM of 25 m spatial resolution: the MDT25 model obtained from the National Geographic Institute of Spain. (<http://centrodedescargas.cnig.es/CentroDescargas/catalogo.do?Serie=LIDA2>). This DEM is represented in Figure 4(c).

The land use data of the Mar Menor watershed was obtained from the Crop and Land Use Map 2000-2010 generated by the Ministry of Agriculture, Fisheries, Food and Environment (MA-PAMA) at a scale of 1:50,000 (https://www.mapa.gob.es/es/cartografia-y-sig/publicaciones/agricultura/mac_2000_2009.aspx). This map corresponds to a nationwide cartography in which crops and land uses are delimited and described using codes. These were reclassified into SWAT land uses. In figure 4(d) there is a representation of this land uses.

Soil data were obtained from the Harmonized World Soil Database (HWSD) (<http://webarchive.iiasa.ac.at/Research/LUC/External-World-soil-database/HTML/>). This Harmonized World Soil Database consists of a 30 arc-second cell database, which includes more than 15,000 soil mapping units and harmonizes regional and national soil data sets of the world (SOTER, ESD, China Soil Map, WISE) with the information contained in the 1:5,000,000 scale FAO-UNESCO World Soil Map.

The compiled raster database consists of 21600 rows and 43200 columns, which are linked to harmonized soil property data. The use of this structure allows the association of attribute data with the raster map for illustration or querying the structure in terms of soil units and characterization of selected soil properties (soil organic carbon, pH, water storage capacity, soil depth, soil cation

exchange capacity and clay fraction, total exchangeable bases, silt and gypsum content, exchangeable sodium percentage, salinity, texture classes and granulometry).

Three slope categories (0-2%, 2-8% and > 8%) were defined and a threshold level of 10% was set to simplify model processing and eliminate slopes, soils and minor land uses used for each subwatershed.

The physical characteristics and land use of the Mar Menor watershed are discussed in the 1.5.2 section.

2.2 Climatic data

The SWAT12 and SWAT+ models need daily meteorological input data such as air temperature, precipitation, wind speed, solar radiation and humidity. With this information, SWAT determines the evapotranspiration that occurs on the watershed. The Hargreaves method is used for the two models described in this report, as a consequence, only temperature and precipitation information are required.

For the meteorological input data for the Lake Erken basin, daily precipitation and temperature data were obtained from the Erken Laboratory meteorological station (59°51'30.7080" N, 18°24'17.5536" E), situated on the Malma islet (Figure 2(c)). This station provides automated measurements of the daily temperature and precipitation data among other information.

The climatic data used in the Mar Menor model was obtained from the Agricultural Information System Network of Murcia (SIAM). The records are evaluated, validated and stored in a server by IMIDA, which can be accessed free of charge from the SIAM website (<https://geoportal.imida.es/siam/>). In the Campo de Cartagena, there are seven weather station that have been used for this model. Figure 4(c) shows the location of all the stations used and table 1 shows information about them.

Table 1. Weather stations in Campo de Cartagena, the Mar Menor basin.

Name	Code	X_UTM	Y_UTM	Height (m)	Municipality
Corvera	CA21	665.200	4.188.754	227	Murcia
Balsapintada	CA42	664.813	4.179.533	138	Fuente Álamo
La Aljorra	CA52	670.129	4.171.693	84	Cartagena
El Campillo	CA91	655.332	4.173.881	175	Fuente Álamo
Sangonera La Verde	MU31	652.257	4.195.930	140	Murcia
La Alberca	MU62	663.907	4.200.807	56	Murcia
Torre Blanca	TP42	685.074	4.182.798	31	Torre Pacheco

2.3 Calibration data

To develop an accurate hydrological model real observed data is required to compare with the output data obtained from running the model. This allows, one, to first develop a model that is as similar to reality as possible, by adjusting the parameters so that the output data are as close as possible to the observed data; and second, to check the reliability of the model. These two processes are known as model calibration and model validation respectively. The calibration and validation of a model is usually logistically limited by the actual data available and the period over which it has been collected.

One of the simplest and therefore most common ways to calibrate a SWAT model is with observed streamflow data at the basin outlet. On the Lake Erken we have daily discharge data that has been measured at Kristineholm, the largest input of the lake. Thanks to the monitoring carried out by the Limnology Department of the Uppsala University, these data are available since mid-2006. For the Lake Erken basin the SWE was also calibrated due to the importance of snow on the water cycle in Sweden. The SWE data were obtained from the Copernicus Global Land Service. It offers a 0.05 spatial resolution, calculated by integrating passive microwave radiometer brightness temperature readings from the Special Sensor Microwave Imager/Sounder with synoptic weather station network snow-depth data (Loujus *et al.*, 2017).

As for the Mar Menor model the calibration of surface hydrology has been carried out using evapotranspiration data. Tobin & Bennett (2017) and Odusanya *et al.* (2019) proved that the AET GLEAM product can be an alternative approach to calibrate the SWAT model. Therefore, due to the unavailability of recorded discharge measurements in the Mar Menor watershed, the satellite-derived AET data from GLEAM were selected as observed inputs. GLEAM is a remote-sensing evapotranspiration dataset developed by the Vrije University of Amsterdam (Miralles *et al.*, 2011). GLEAM includes a set of algorithms that estimate the different components of terrestrial evaporation (i.e., transpiration, bare soil evaporation, sublimation, interception loss and open-water evaporation) and root-zone soil moisture from satellite data. The last version of GLEAM (v3) has been globally validated through 91 eddy-covariance towers and 2325 in situ sensors (Martens *et al.*, 2017). In this study, the AET data of version 3.2b of GLEAM was implemented. This dataset is available on a 0.25°-latitude-longitude regular grid.

Since our goal is to obtain output data related to the sediment and nutrients that enters the lakes, it was also planned to calibrate the concentration of these two elements in the water discharge, but for this it was first necessary to have a good calibration of the hydrology of the basin. Work is currently underway on sediment and nutrient calibration of both models. Although some data regarding sediment and nutrient discharge have already been obtained from the Erken model, they have not yet been optimized through calibration.

3. Development of the models

3.1 Sub-basin delimitation

To develop a SWAT12 or SWAT+ model the first step is to divided the watershed in sub-basins, and each sub-basin into HRUs. QSWAT and QSWAT+ performs this process through the integration and combination of the spatial data described in section 2.2.1, being each HRUs the result of a unique combination of land use, soil and elevation. For the SWAT+ model developed for Lake Erken, the watershed was divided in 12 sub-basin that are represented in Figure 2(b). For the SWAT12 model developed for the Mar Menor, the watershed was divided in 20 different sub-basins that are represented in Figure 4(b). A bigger watershed is generally divided in more sub-basin due to the diversification of land uses and soil types in the same basin, as well as the greater geographic variety. Although this is the case between the two basins studied, this need not always happen.

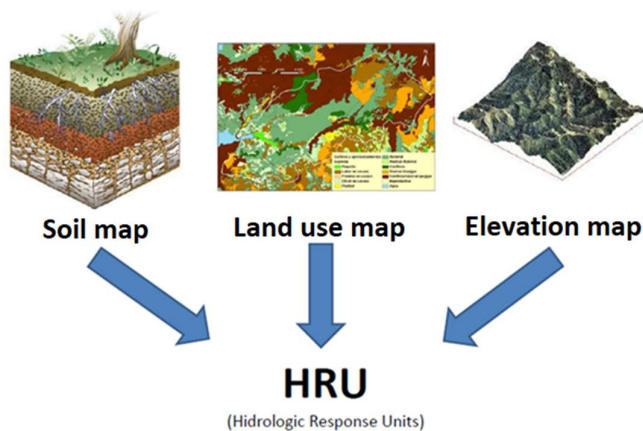


Figure 6. Scheme for the SWAT creation of HRUs.

3.2 Sensitivity analysis, calibration and validation

To obtain results with SWAT there are three main steps. First, to locate the most influential parameters effecting the streamflow or other data we are calibrating, by performing a sensitivity analysis. Second, to adjust the sensitive parameters with an automatic calibration using the real data describe in section 2.3 for a concrete period. Finally, to use the same data but for a non-calibrated period to validate the SWAT model. The methodology of these three steps is described below.

In the SWAT12 and SWAT+ model, there is a multitude of calibration parameters, and, to avoid over-parameterization and identify the most sensitive parameters in the hydrological process of our study areas, a sensitivity analysis was executed (Arnold *et al.*, 2012) before the calibration and validation processes. Sensitivity analysis determines how much changes in model parameters affect model outputs. It is a necessary process to identify the key parameters needed for calibration, and to select those parameters that have a significant impact on model outputs of interest.

Model calibration is the process of estimating the value of the parameters by comparing the model simulation outputs with the observed data for the same conditions. Automatic calibration optimizes

the parameter values using numerical methods. This calibration involves the calculation of the prediction error using an equation called objective function, and an automatic optimization procedure using a search algorithm. This algorithm searches for the parameter values that optimize the objective function value (Gupta, Sorooshian & Yapo, 1999). In the case of the SWAT model, with a large number of parameters and complex operation, automatic calibration is the calibration method of choice.

The results of the simulations depend on the state of the system at time zero, so special care must be taken when choosing these conditions. For this purpose, the warm-up period is used, which consists of an initial period (2-5 years) for the model to stabilize and adjust correctly to the local conditions and thus improve the quality of the simulation.

For the SWAT+ Lake Erken model, the sensitivity analysis and automatic calibration were performed in Toolbox (Chawanda, 2021), a free software designed to perform SWAT+ model sensitivity analysis, calibrations, and more. For the sensitivity analysis, Toolbox uses the Sobol method (Sobol, 2001). Within an ensemble, it divides the overall output variance into the variation produced by each parameter. For the automatic calibration, Toolbox uses a dynamically dimensioned search (DDS). The Nash-Sutcliffe efficiency coefficient was applied as the objective function in this investigation. A total of 500 simulations were run. After this first interaction the results were satisfactory, and no other interaction was required.

For the SWAT12 models, the sensitivity analysis and automatic calibration were carried out using the Sequential Uncertainty Fitting procedure (SUFI-2) included in the SWAT Calibration and Uncertainty Programs (SWAT-CUP) (Abbaspour, 2013). For the SWAT+ Mar Menor model, there is a SWAT+ Calibration and Uncertainty Programs (SWATplus-CUP). Instead of SUFI-2, it used the Swat Parameters Estimator (SPE), that works in a similar way. For the automatic calibration process carried out in SWAT_CUP and SWATplus_CUP, the Kling-Gupta efficiency index (KGE) (Gupta *et al.*, 2009) (Eq. 1) was set as the objective function.

Equation 1. Kling-Gupta efficiency index.

$$KGE = 1 - \sqrt{(\alpha - 1)^2 + (\beta - 1)^2 + (\gamma - 1)^2}$$

Where α is the Pearson correlation coefficient between the observed and simulated data, β is the fraction of standard deviation of the simulated data over the observed data and γ is the average simulated value over the average observed value. KGE ranges from $-\infty$ to 1, with 1 being the optimal value.

And finally, the validation process consists of running the model outside of the calibration period using the parameters determined in the calibration to demonstrate that the model is sufficiently accurate for the case study (Moriasi *et al.*, 2007). The validation process involved the introduction of the fitted parameters obtained during the calibration process to the SWAT model and the comparison between the real data and SWAT-simulated data.

The length of these periods (calibration and validation) is estimated depending of the total years of real data available. The longer the calibration period, the more the parameters can be adjusted to the specific model. However, a sufficient validation period must also be provided to check the effectiveness of the model. Discounting the warm-up period, which can range from 2 to 5 years, the years of observed data are usually divide into 2/3 for calibration and 1/3 for validation. Another option is to dived them into 1/2 and 1/2.

3.3. Evaluation of the models

The goodness of fit for each calibration and validation was determined using Moriasi's four recommended statistics. In other words, for both calibration and validation, the performance of the models was evaluated using Moriasi's four recommended statistics (Moriasi *et al.*, 2015). These statics are described below.

The coefficient of determination (R^2) (Eq. 2), indicates the proportion of the variance of the measured data that can be explained by the model. R^2 ranges between 0 and 1, the higher the value the lower the variance error, values above 0.5 are considered acceptable (Moriasi *et al.*, 2007).

Equation 2. Coefficient of determination.

$$R^2 = \left[\frac{\sum_{i=1}^n (O_i - \bar{O}) (S_i - \bar{S})}{\sqrt{\sum_{i=1}^n (O_i - \bar{O})^2} \sqrt{\sum_{i=1}^n (S_i - \bar{S})^2}} \right]^2$$

The Nash-Sutcliffe efficiency (NSE) (Eq. 3) (Nash & Sutcliffe, 1970) is a standardized statistic that determines the relative magnitude of the residual variance versus the variance of the observed data. NSE ranges from $-\infty$ to 1, with the optimal value being $NSE=1$. Values between 0 and 1 mean acceptable performance, while values below 0 indicate that the observed mean value is a better predictor than the simulated value, indicating unacceptable performance (Moriasi *et al.*, 2007).

Equation 3. Nash-Sutcliffe efficiency.

$$NSE = 1 - \frac{\sum_{i=1}^n (O_i - S_i)^2}{\sum_{i=1}^n (O_i - \bar{O})^2}$$

The standard deviation of measured data (RSR) (Eq. 4), is an index commonly used to quantify the error in the estimation in the same units as the data. It is calculated with the following equation:

Equation 4. Standard deviation.

$$RSR = \frac{\sqrt{\sum_{i=1}^n (O_i - S_i)^2}}{\sqrt{\sum_{i=1}^n (O_i - \bar{S})^2}}$$

And, lastly, the percent bias (PBIAS) (Eq. 5). PBIAS is the average tendency of the simulated data to be larger or smaller than their observed counterparts. The optimum value of PBIAS is 0, values of low magnitude indicate an accurate model simulation.

Equation 5. Percent bias.

$$\text{PBIAS} = \frac{\sum_{i=1}^n (O_i - S_i)}{\sum_{i=1}^n O_i} \times 100$$

In equations 2, 3, 4 and 5, the observed and simulated data are O_i and S_i respectively; the average observed and simulated values are \bar{O} and \bar{S} ; and n refers to the total number of data points

4. Results

The models have been developed with the spatial data and meteorological data. In this section we explain and show different results obtained. First, we show and discuss the results of the calibration and validation of different output data from each model. Once the effectiveness of the models has been proven, through the calibration and validation, we present different results. On one hand, we obtain a description of the water balance of each of the modeled basins from the direct application of SWAT+. On the other hand, SWAT models can be applied and have been applied for many different purposes, which further exemplify their usefulness. In the Lake Erken basin, the SWAT+ model was successfully used to predict changes on the water balance under different climatic scenarios, i.e., as a long-term prediction tool (Jiménez-Navarro *et al.*, 2021).

In this section the parameters used for calibration are discussed and the statistics obtained from the calibration and validation are shown. In addition, we discuss the water balance of each modeled basin. The SWAT and SWAT+ software has SWATCHECK, which returns the total mean of the main components of the generated model. This allows a rapid estimation of the different cycles simulated by the model. SWATCHECK graphically and schematically represents the annual average of the main components of the hydrological cycle of each modeled watershed.

4.1 SWAT12 Lake Erken model

4.1.1 Warm-up, calibration and validation periods

The calibration and validation periods of a model are limited by the available observed data. The warm-up period consists of leaving a series of initial years for the model to adjust correctly to reality and thus improve the quality of our simulation. In this study a warming period has been applied since both the SWAT model and the SWAT+ model require it for the simulation of the basin. We divided the calibration and validation period in 2/3 and 1/3 for the Lake Erken model. Table 2 specifies the periods used for the Lake Erken basin.

Table 2. Warm-up, calibration and validation periods for Lake Erken model.

Phase	Period	Total years
Warm-up	2005-2006	2
Calibration	2007-2015	9
Validation	2016-2020	5

4.1.2 Streamflow calibration and validation

There are near 200 parameters in the SWAT and SWAT+ model, a large part of them can affect the streamflow. Many are well known parameters that are closely related to water discharge. We perform a sensitivity analysis with these parameters in order identify and calibrate only the more sensitives ones. The Sobol sensitivity analysis found 11 parameters that are sensitive for this model: *cn2*, *alpha*, *esco*, *perco*, *revap_co*, *epco*, *awc*, *flo_min*, *revap_min*, *surlag* and *k*. Table 3 show the modified parameters along with their range and the final value after the calibration.

Table 3. Range and adjusted value of all modified streamflow parameters after the calibration.

Parameter	Range	Adjusted value
CN2	-20%-20%	-18%
ALPHA	0-1	0.35
ESCO	0 -1	0.50
GWQMN	0-5000	0.001
GW_REVAP	0.02-0.2	0.05
EPCO	0-1	0.50
SOL_AWC	-20%-20%	12.62%
SOL_K	-20%- 20%	-9.82%
REVAPMN	0-1000	1313.18
SURLAG	0.05-24	1.20

A description of these parameters, along with the rest of SWAT and SWAT+ parameters relevant for the models described on this report, can be found in appendix I.I.

Concurring with Cibin, Sudheer & Chaubey (2010), most of the parameters that have a major effect on the streamflow reenactment, are sensible parameters in our region. The parameters related to the land slope are not sensible, since this watershed does not display noteworthy changes in elevation, nor are the parameters related to the horizontal stream. In this region the most relevant parameters appear to be related to the groundwater and aquifers (*alpha*, *revap_co*, *flo_min*, *revap_min*) and to the soil (*cn2*, *esco*, *perco*, *awc*, *k*). A few soils qualities impact groundwater resistance, which warrants the consideration of soil parameters as valuable. These parameters are commonly utilized in different works (Molina-Navarro *et al.*, 2014).

Table 4. Calibration and validation of the streamflow statistical daily values.

Period	NSE	PBIAS	RSR	R ²
Calibration	0.48	-6.67%	0.72	0.58
Validation	0.48	-29.52%	0.72	0.58

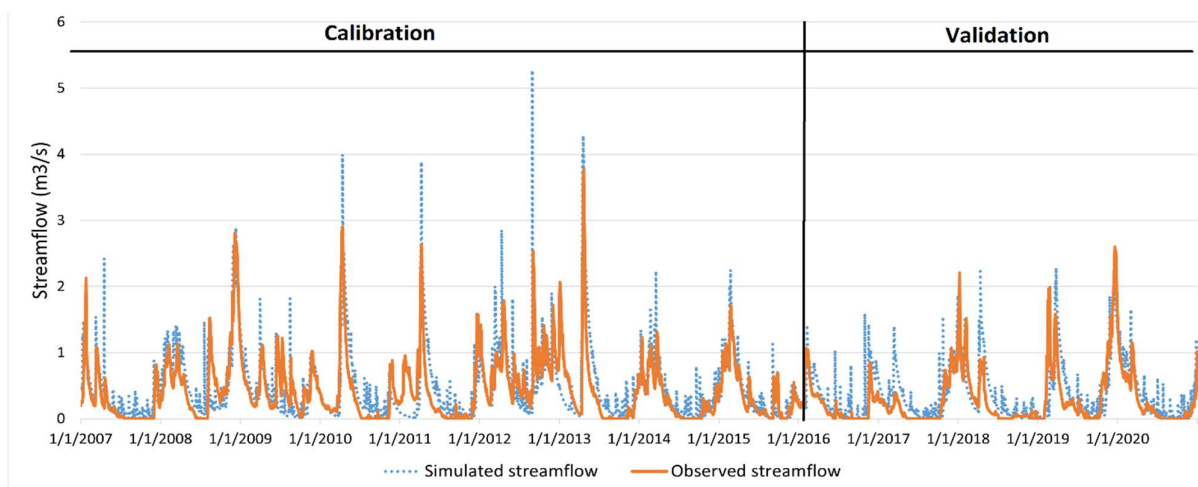


Figure 7. Daily calibration and validation of the SWAT+ model streamflow.

The reliability of the hydrology of the developed model is ratified both by the statistics recommended by Moriasi *et al.* (2015) (table 4) and by the graphical comparison of the actual water discharge and the discharge simulated by the model at Kristineholm (Figure 7).

The SWAT12 model responded adequately for both the calibration and validation period, according to the statistical evaluation indices provided in Table 4. Nevertheless, with the SWAT+ model we obtained better results calibrating the same parameters (section 4.2)

4.1.3 Water balance of the Lake Erken watershed

The water balance of the Lake Erken watershed is graphically represented in Figure 8.

According to SWATCHECK (figure 8), the Lake Erken watershed has a positive balance, since the amount of water that precipitates (581.8mm) is greater than the amount of water lost through evapotranspiration (439.1mm), even though the evapotranspiration is really high in the basin (75.47% of the precipitation). The water percolation to the shallow aquifer is significant in the basin, but the return flow from the aquifer to the lake is also quite high. The water flowing down to the deep aquifer is minimal. As for the water that enters Lake Erken, most of it enters as the return flow. The lateral flow, that is, the water that enter the lake trough the channels, is not so high but still very significant. On the other hand, the water that enters as surface runoff after a precipitation is minimal.

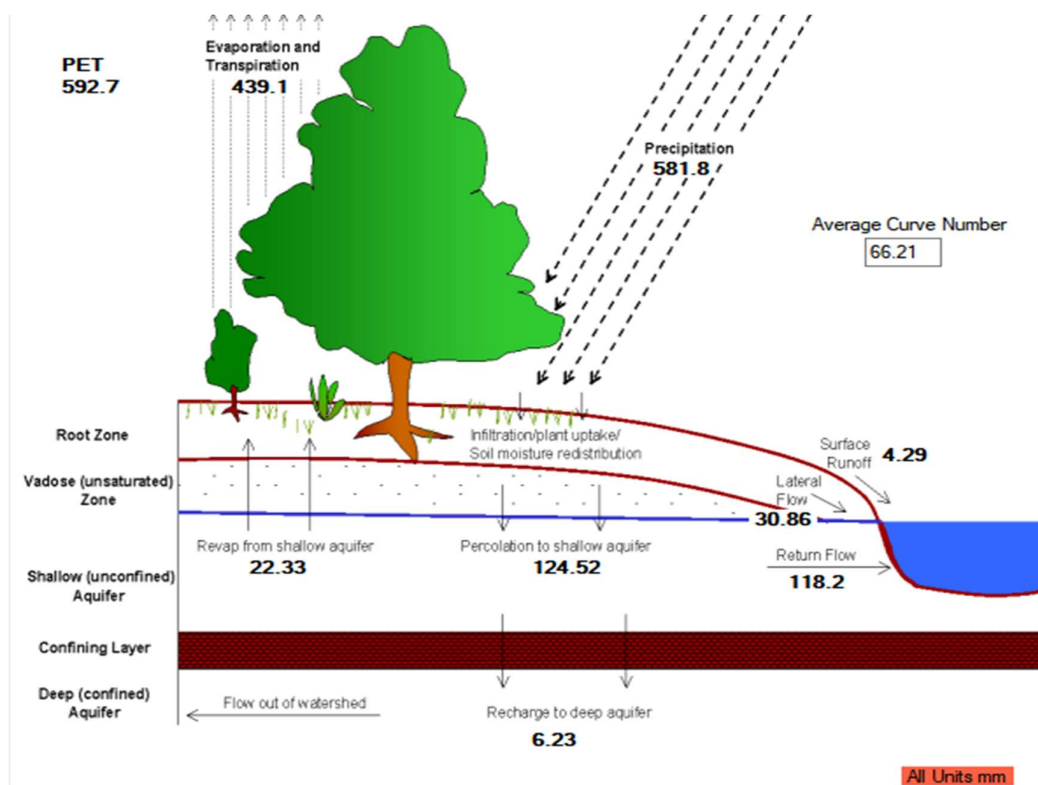


Figure 8. The water balance of the Lake Erken watershed. All units are mm.

4.2 SWAT+ Lake Erken model

For the Lake Erken SWAT+ model the main calibration was done based on the comparison of simulated and measured streamflow data. With these data we enhance the hydrology of the model. In addition, since the snow is relevant component of the hydrological cycle in Sweden, a complementary manual calibration of the snowpack has been performed. With this we obtain a more realistic and complete SWAT+ model. A future addition to this model will be the calibration of others components such as sediments and nutrients present in the water flow and entering the lake.

4.2.1 Warm-up, calibration and validation periods

The calibration and validation periods of a model are limited by the available observed data. The warm-up period consists of leaving a series of initial years for the model to adjust correctly to reality and thus improve the quality of our simulation. In this study a warming period has been applied since both the SWAT model and the SWAT+ model require it for the simulation of the basin. We divided the calibration and validation period in 2/3 and 1/3 for the Lake Erken model. Table 5 specifies the periods used for the Lake Erken basin.

Table 5. Warm-up, calibration and validation periods for Lake Erken model.

Phase	Period	Total years
Warm-up	2005-2006	2
Calibration	2007-2015	9
Validation	2016-2020	5

4.2.2 Streamflow calibration and validation

There are near 200 parameters in the SWAT and SWAT+ model, a large part of them can affect the streamflow. There are well known parameters that are closely related to water discharge. We perform a sensitivity analysis with these parameters in order to calibrate only the more sensitive ones. The Sobol sensitivity analysis found 11 parameters that are sensitive for this model: *cn2*, *alpha*, *esco*, *perco*, *revap_co*, *epco*, *awc*, *flo_min*, *revap_min*, *surlag* and *k*.

Table 6 show the modified parameters along with their range and the final value after the calibration.

Table 6. Range and adjusted value of all modified streamflow parameters after the calibration.

Parameter	Range	Adjusted value
Cn2	-20%-20%	-18%
Alpha	0-1	0.35
Esco	0 -1	0.50
Perco	-0.05-0.05	0.001
Revap_co	0-1	0.05
Epco	0.01-1	0.50
Awc	-20%-20%	-0.5%
Flo_min	0-5000	230.08
Revap_min	0-5000	1313.18
Surlag	1-24	1.20
K	1-100	99.77

A description of these parameters, along with the rest of SWAT and SWAT+ parameters relevant for the models described on this report, can be found in appendix I.I.

Most of the parameters had optimized values within the anticipated range for a watershed within the Scandinavian peninsula, and the parameters *cn2*, *esco*, *perco* and *snomelt_tmp* are the most excellent fitted to the anticipated values (Malagò *et al.*, 2015).

Table 7. Calibration and validation of the streamflow statistical daily values.

Period	NSE	PBIAS	RSR	R ²
Calibration	0.7073	0.6192%	0.5410	0.7143
Validation	0.7704	-19.3319%	0.4791	0.7945

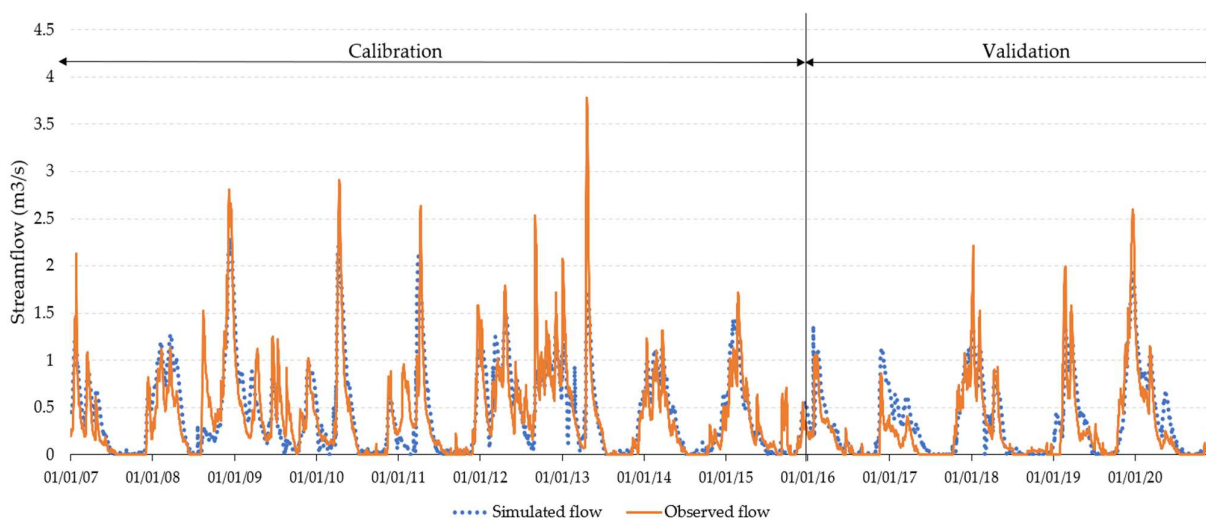


Figure 9. Daily calibration and validation of the SWAT+ model streamflow.

The reliability of the hydrology of the developed model is demonstrated both by the statistics recommended by Moriasi *et al.* (2015) (table 7) and by the graphical comparison of the actual water discharge and the discharge simulated by the model at Kristineholm (Figure 9).

Precipitation was low during the validation period compared to the calibration period, which means streamflow was likewise low in those years. The average annual precipitation during the calibration period (2007–2015) is over 600 mm, while the average annual precipitation for the validation period (2016–2020) is below 550 mm. The negative value of the PBIAS statistic implies that the simulated streamflow was exaggerated, even though it was still within acceptable bounds. The model eventually overestimated the streamflow discharge during dry times because the calibration period was wetter than the validation period. Despite this, the statistics are satisfactory, implying that the model is applicable during both dry and wet seasons. The SWAT+ model responded adequately to this change, according to the statistical evaluation indices provided in Table 7.

4.2.3 Snowpack calibration and validation

Snow is a significant component of the climate and the hydrologic cycle in the south of Sweden, as it is in any geographical area near the poles (Adam, Hamlet & Lettenmaier, 2009). During the cold season, all basins are partially covered by snow. As a result, the hydrological cycle is heavily influenced by snowfall, snow accumulation, and snow melting (Tarboton *et al.*, 1994). Changes in the estimation of these water balance components can have a considerable impact on a hydrological simulation (Zeinivand, & De Smedt, 2009). As a consequence, when modeling snow-covered basins, researchers should take these factors into account (Grusson *et al.*, 2015). The SWE and snowmelt are the most important snow statistics. The SWE is defined as a water column formed by the melting of unit cross-section snow samples with a height equal to the snowpack depth at the measurement point (Paul *et al.*, 1994). The SWE is the most important factor in determining the volume of snowmelt runoff. In snow runoff analysis, it is used as a variable to estimate the distribution and quantity of snow (Pradhanang *et al.*, 2011).

To enhance the model, we performed a manual calibration of the SWE with the snow-related parameters. This calibration has been done on a monthly scale. Since Toolbox does not allow for calibrating the SWE, we performed the calibration manually in SWAT+ Editor, which is a tool for editing, running, and saving changes to a SWAT model. Then, we validated each test in a spreadsheet by applying equations (2, 3, 4 and 5) to the snowpack data. In the end, we calibrated manually five snow parameters: snowfall_tmp, snomelt_min, snomelt_max, snomelt_tmp and snomelt_lag.

After the calibrations, only the modification of two parameters enhanced the simulation of SWE in the model: snomelt_tmp and snomelt_lag, the rest of the parameters were left with their default values (Table 8).

Table 8. Range and adjusted value of snowpack parameters after the calibration.

Parameter	Range	Adjusted value
Snofall_tmp	-5°C - 5°C	1°C
Snomelt_tmp	-5°C - 5°C	0°C
Snomelt_max	1.4 - 8.0	4.5
Snomelt_min	1.4 - 8.0	4.5
Snomelt_lag	0.01 - 1	0.2

A description of these parameters, along with the rest of SWAT and SWAT+ parameters relevant for the models described on this report, can be found in appendix I.I.

Table 9. Monthly calibration and validation of the snowpack statistical values.

Period	NSE	PBIAS	RSR	R ²
Calibration	0.7322	-3.0326%	0.5175	0.8436
Validation	0.8879	13.65352%	0.3349	0.9072

Both the calibration and validation periods return very satisfactory results for the statistics proposed by Moriasi *et al.* (2015) (table 9). Figure 10 shows the visual comparison of the snowpack simulated by the SWAT+ model with the real snow water equivalent obtained by satellite. The graph shows how the SWAT+ model simulates the snow accumulation in the Lake Erken watershed realistically and reliably both in years where snow accumulation is very large (2013, 2014) and in years where this accumulation is less pronounced (2011, 2013). Thus, we can be confident that the predictions made with this model about snow accumulation in the basin will be more or less realistic.

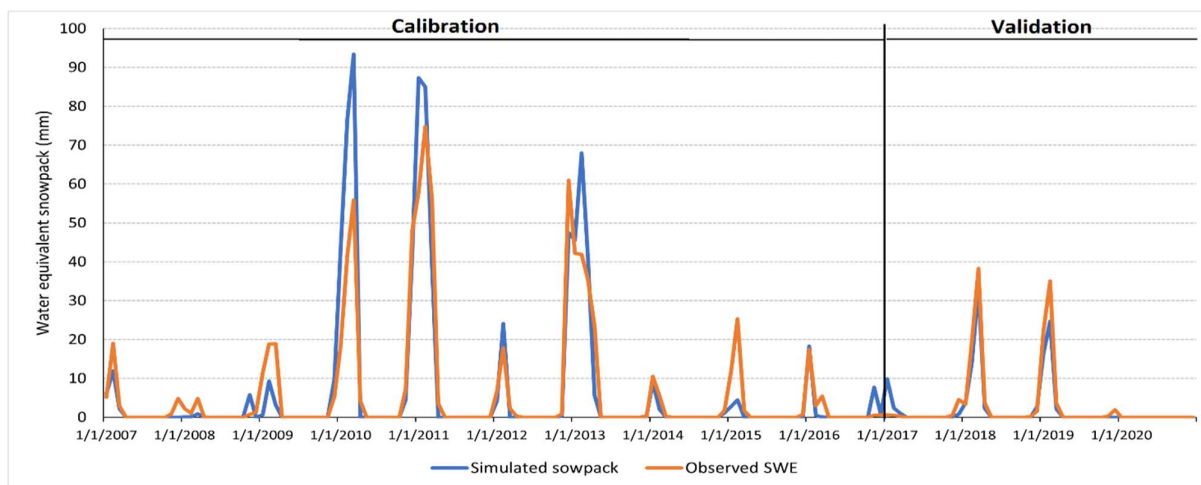


Figure 10. Monthly calibration and validation of the SWAT+ model snowpack.

4.2.4 Sediment and nutrients future calibration

The latest version of SWAT+ features many important improvements in sediment and nutrient performance. However, this version was released on March 31 of this year (2022), so the Lake Erken model presented in this report does not have these improvements. In addition, the latest toolbox version also allows to calibrate both sediments and different types of nutrients (organic nitrogen, nitrate, nitrite, ammonium, organic phosphorus and mineralized phosphorus). Although there has not yet been time to fully develop a new model with these new constituents, we have already performed sensitivity analyses to know which parameters related with these outputs tend to be sensitive, in order to calibrate them in the near future.

For the sediments we calibrate seven parameters: *cherod*, *cov*, *spcon*, *spexp*, *usle_p*, *usle_k*, and *prf*. Out of these parameters only *spcon* and *spexp* present 0 sensibility and they have been discarded for future calibration (Table 7).

We found eleven nitrogen related parameters: *cdn*, *cmn*, *erorgn*, *no3*, *nperco*, *nstlr1*, *nstlr2*, *n_updis*, *rsdco*, *sdnco* and *lat_orgn*. There are six sensitive parameters according with the Sobol sensitivity analysis: *cdn*, *erorgn*, *nperco*, *n_updis*, *sdnco* and *lat_orgn* (Table 7).

And lastly, we found eight phosphorus related parameters: *erorgp*, *psetlr1*, *psetlr2*, *pperco*, *phoskd*, *psp*, *p_updis*, *lat_orgp*. Five of these parameters presented a sensitivity different to 0, and are going to be calibrated: *erorgp*, *phoskd*, *psp*, *p_updis* and *lat_orgp* (Table 10).

A description of these parameters, along with the rest of SWAT and SWAT+ parameters relevant for the models described on this report, can be found in appendix I.I.

Table 10. Range of sensitive parameters for the sediment, nitrogen and phosphorus calibration.

Calibration	Parameter	Range
Sediment	Cherod	0 - 1
	Cov	0 - 1
	Usle_p	0 - 1
	Usle_k	-0.2 - 0.2
	Prf	0 - 2
Nitrogen	Cdn	0 - 3
	Erorgn	0 - 5
	Nperco	0 - 1
	N_updis	1 - 31
	Sdnco	0 - 1
	Lat_orgn	0 - 200
Phosphorus	Erorgp	0 - 5
	Phoskd	100 - 200
	Psp	0 - 0.7
	P_updis	0 - 100
	Lat_orgp	0 - 200

4.2.5 Water balance of the Lake Erken watershed

The water balance of the Lake Erken watershed is graphically represented in Figure 11.

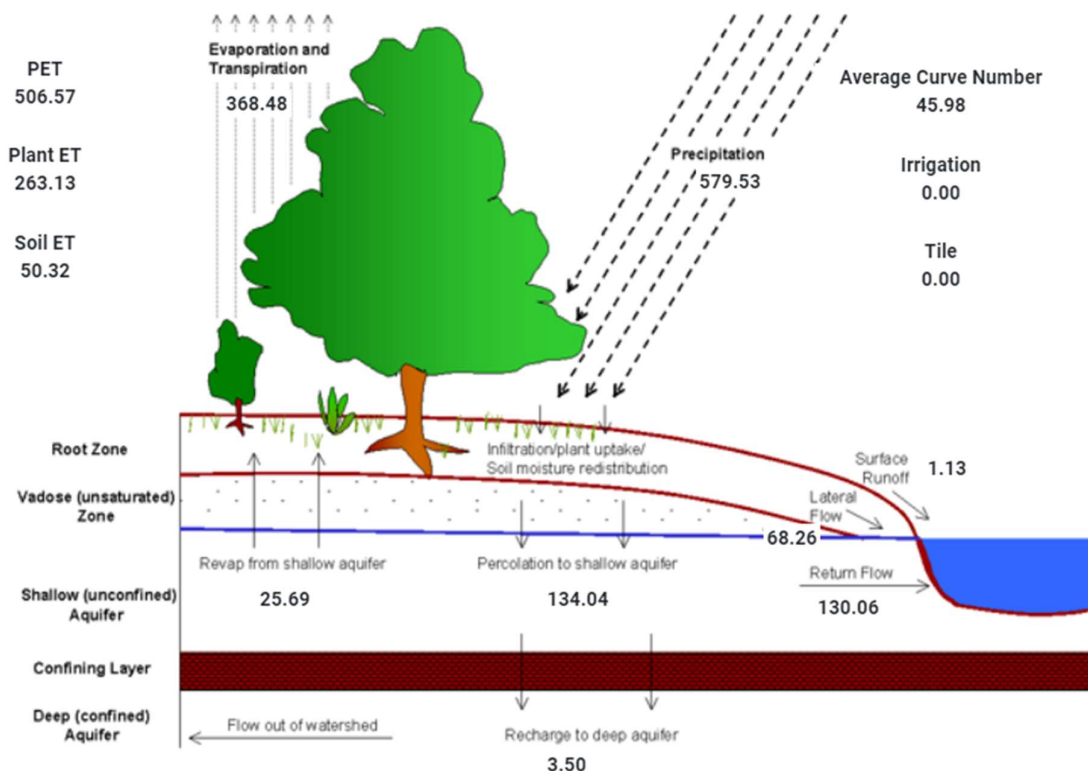


Figure 11. The water balance of the Lake Erken watershed. All units are mm.

According to SWATCHECK (figure 11), the Lake Erken watershed has a positive balance, since the amount of water that precipitates (579.53mm) is greater than the amount of water lost through evapotranspiration (368.48mm), even though the evapotranspiration is quite high in the basin (63.58% of the precipitation). The water percolation to the shallow aquifer is significant in the basin, but the return flow from the aquifer to the lake is also quite high. The water flowing down to the deep aquifer is minimal. As for the water that enters Lake Erken, most of it enters as the return flow. The lateral flow, that is, the water that enter the lake through the channels, is not so high but still very significant. On the other hand, the water that enters as surface runoff after a precipitation is minimal. This model has been used to predict changes in the hydrological cycle (Jiménez-Navarro *et al.*, 2021).

4.3 SWAT12 Mar Menor model

4.3.1 Warm-up, calibration and validation periods

The warm-up period consists of leaving a series of initial years for the model to adjust correctly to reality and thus improve the quality of our simulation. In this study a warming period has been applied since both the SWAT model and the SWAT+ model require it for the simulation of the basin. We divided the calibration and validation period in 1/2 and 1/2 for the Mar Menor model. Table 11 specifies the periods used for the Mar Menor basin.

Table 11. Warm-up, calibration and validation periods for Mar Menor model.

Phase	Period	Total years
Warm-up	2000-2002	3
Calibration	2003-2009	7
Validation	2010-2016	7

4.3.2 Evapotranspiration calibration and validation

An accurate knowledge of evapotranspiration is necessary for the study of the water resources available in a basin. In the Mar Menor watershed model the Penman-Monteith method was used to calculate the potential evapotranspiration required by SWAT. Potential evapotranspiration (PET) is the evapotranspiration that would occur on a surface uniformly covered with vegetation, at a time of growth, with unlimited access to soil moisture and without being exposed to adverse weather conditions.

Based on the literature reviewed (Oduşanya *et al.*, 2019), (Ha *et al.*, 2018), (Tobin & Bennett, 2017), (Sun & Ren, 2013), 12 of the most frequently used parameters for AET calibration were selected for a global sensitivity analysis. Parameter sensitivity was calculated on the basis of the significance of the sensitivity (p-value); the lower the p-value, the more sensitive the parameter (Abbaspour, 2013). After sensitivity analysis, ALPHA_BF and the seven most sensitive parameters (ESCO, CN2, EPCO, SOL_BD, CANMX, SOL_AWC and SOL_K) and were chosen for automatic calibration. The result of this calibration is shown in table 12.

Table 12. Range and adjusted value of snowpack parameters after the calibration.

Parameter	Range	Adjusted value
Esco	0 – 1	0.86
Cn2	-20% - 20%	-7.24%
Epc0	0 - 1	0.14
Sol_bd	-20% - 20%	-8.2%
Canmx	0 - 100	12.1
Awc	-20% - 20%	14.84%
K	-20% - 20%	-5.32%
Alpha	0 - 1	0.16

A description of these parameters, along with the rest of SWAT and SWAT+ parameters relevant for the models described on this report, can be found in appendix I.I.

Table 13. Monthly calibration and validation of the AET statistical values.

Period	NSE	PBIAS	KGE	R ²
Calibration	0.67	-9.11%	0.81	0.73
Validation	0.71	-5.22%	0.82	0.74

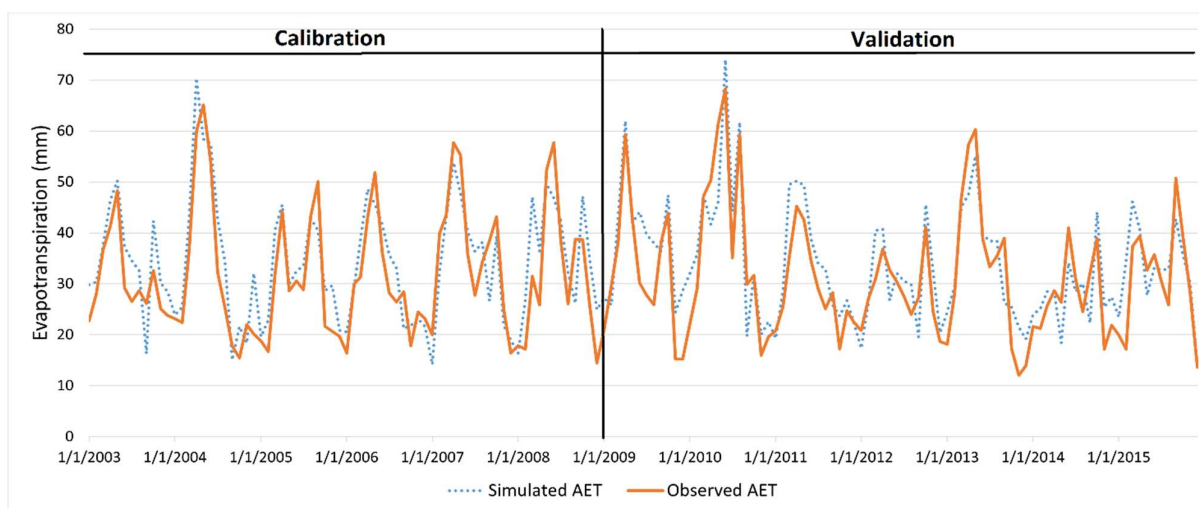


Figure 12. Comparison of monthly observed and simulated AET.

The table 13 shows that the SWAT model of the Mar Menor basin had a good performance both in calibration and validation period for AET simulation at a monthly basis according to the statistics criteria proposed by Moriasi *et al.* (2015) and Kouchi *et al.* (2017). Figure 12 shows the graphical performance of SWAT by comparing simulated AET with observed AET values obtained from GLEAM at watershed scale. These graphical results indicate a satisfactory performance of SWAT to simulate the AET magnitude and trends.

4.3.3 Water balance of the Mar Menor watershed

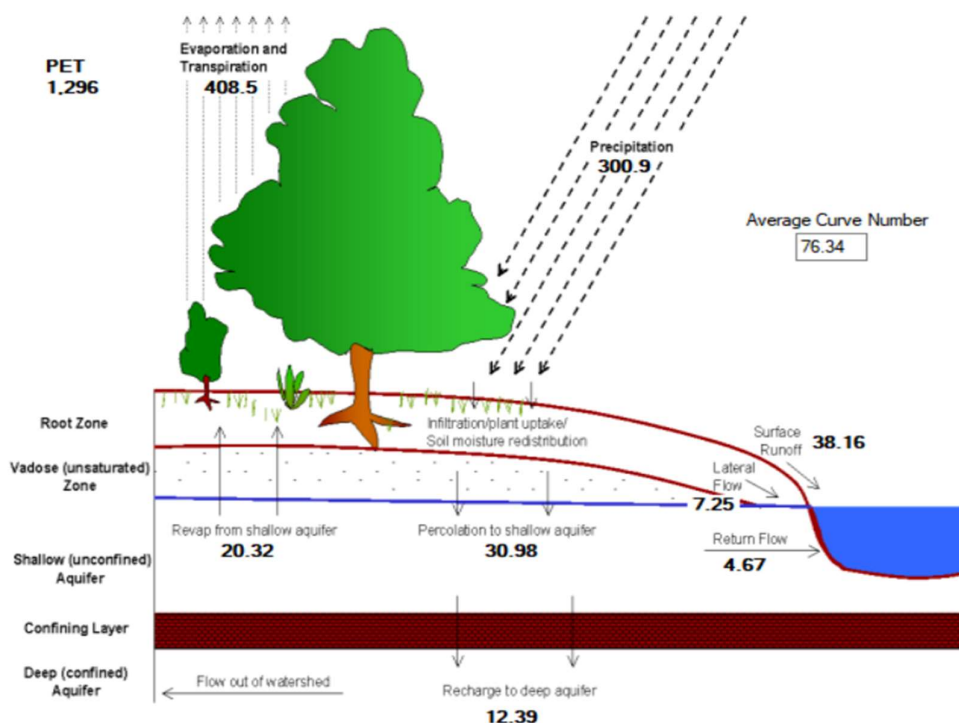


Figure 13. The water balance of the Lake Mar Menor watershed. All units are mm.

The annual water balance of the Mar Menor watershed for the period 2003–2019 is shown in figure 13. The average annual rainfall is about 300 mm, supplemented by about 200 mm from other sources that allow crop irrigation in the area. As it was expected, the semiarid climate of the study area and their intensive agriculture make AET the main component to water loss from the basin, with average values above 400 mm. It was also found that the average surface runoff (38.16 mm) is higher than the lateral flow. This is due to the fact that rainfall in Murcia is seasonal and torrential, generating a large amount of surface runoff. On the other hand, there are long periods without rainfall, in which the amount of water that enters the Mar Menor through the basin is minimal. The return flow from the shallow aquifer to the lagoon is also low (4.67mm), since a large part of the water that percolates into the quaternary aquifer connects to the aquifers below (Jiménez-Martínez *et al.*, 2016). The results obtained for the different components of the water balance are in line with those obtained recently by Puertes *et al.* (2021) in their hydrological modelling of the ephemeral streams located to the south of the Albujión stream.

4.3 SWAT+ Mar Menor model

4.4.1 Warm-up, calibration and validation periods

The warm-up period consists of leaving a series of initial years for the model to adjust correctly to reality and thus improve the quality of our simulation. In this study a warming period has been applied since both the SWAT model and the SWAT+ model require it for the simulation of the basin.

We divided the calibration and validation period in the Mar Menor model. Table 14 specifies the periods used for the Mar Menor basin.

Table 14. Warm-up, calibration and validation periods for Mar Menor model.

Phase	Period	Total years
Warm-up	2000-2002	3
Calibration	2003-2009	7
Validation	2010-2015	6

4.4.2 Evapotranspiration calibration and validation

This model is still being calibrated and improved, but a first calibration has already been carried out with the following parameters:

Table 15. Range and adjusted value of snowpack parameters after the calibration.

Parameter	Range	Adjusted value
Esco	0 – 1	0.05
Cn2	-30% - 30%	5.29%
Epc0	0 – 1	0.06
Awc	-30% - 30%	-7.16%
Perco	0 – 1	0.50

A description of these parameters, along with the rest of SWAT and SWAT+ parameters relevant for the models described on this report, can be found in appendix I.I.

Table 16. Monthly calibration and validation of the AET statistical values.

Period	NSE	PBIAS	KGE	R ²
Calibration	0.61	-8.16%	0.78	0.67
Validation	0.61	-4.07%	0.77	0.64

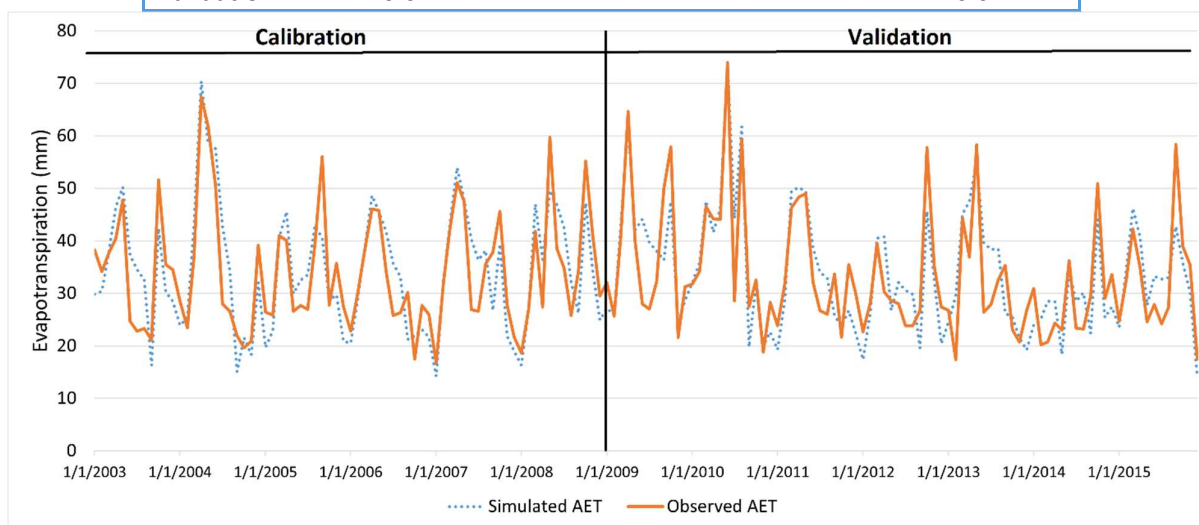


Figure 14. Comparison of monthly observed and simulated AET .

The table 16 shows that the SWAT model of the Mar Menor basin had a good performance both in calibration and validation period for AET simulation at a monthly basis according to the statistics criteria proposed by Moriasi *et al.* (2015) and Kouchi *et al.* (2017). Figure 14 shows the graphical performance of SWAT by comparing simulated AET with observed AET values obtained from GLEAM at watershed scale. These graphical results indicate a satisfactory performance of SWAT to simulate the AET magnitude and trends and are really similar at the ones obtained with the SWAT12 model (section 4.3).

4.4.3 Water balance of the Mar Menor watershed

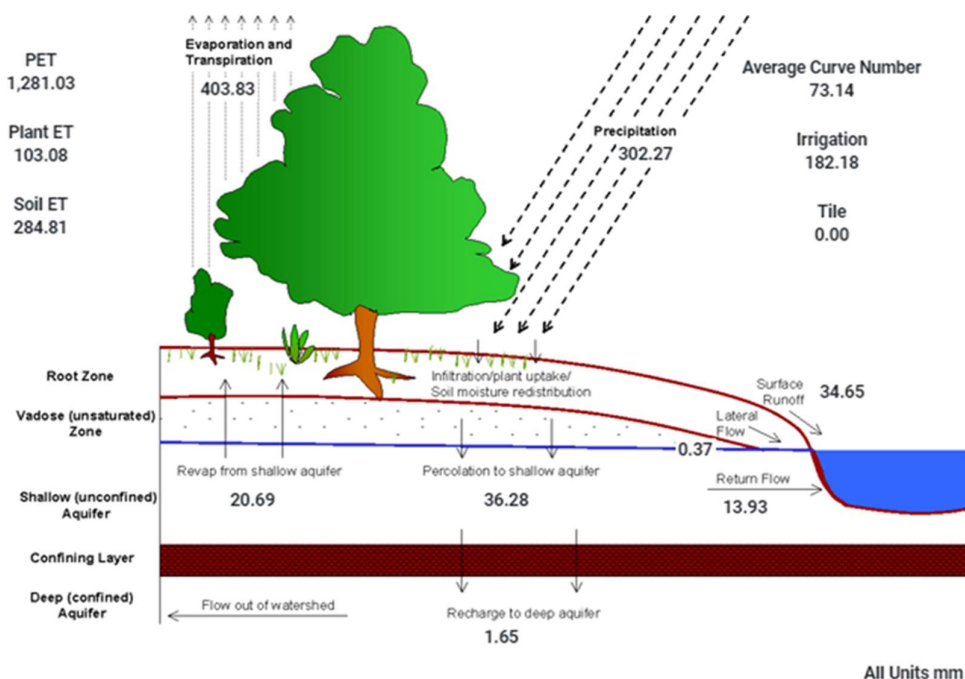


Figure 85. The water balance of the Lake Mar Menor watershed. All units are mm.

The annual water balance of the Mar Menor watershed for the period 2003–2019 is shown in figure 15. The average annual rainfall is about 300 mm. As it was expected, the semiarid climate of the study area and their intensive agriculture make AET the main component to water loss from the basin, with average values above 400 mm. It was also found that the average surface runoff (34.65 mm) is higher than the lateral flow. This is due to the fact that rainfall in Murcia is seasonal and torrential, generating a large amount of surface runoff. On the other hand, there are long periods without rainfall, in which the amount of water that enters the Mar Menor through the basin is minimal. The return flow from the shallow aquifer to the lagoon is also low (13.93mm) but significantly larger than that obtained with SWAT12. Still the percolation is really high, since a large part of the water that percolates into the quaternary aquifer connects to the aquifers below (Jiménez-Martínez *et al.*, 2016). The results are really similar between SWAT12 and SWAT+.

5. Conclusions

In this work, the hydrological basin of the Mar Menor (Cartagena area) and the hydrological basin of Lake Erken have been modeled by means of the SWAT hydrological model and the SWAT+ model. For this purpose, it has been necessary to collect the information needed for the implementation of the model: meteorological information (precipitation and temperature), spatial information (digital terrain model, land use map and soil map), as well as real observed data of the components of the hydrological cycle needed to calibrate and validate the models. The hydrological cycle of the Mar Menor, characterized by its high degree of anthropization and the absence of specific flow information, has been calibrated using real evapotranspiration data from remote sensing. The Lake Erken basin, for which there is a historical record of water discharge, has been calibrated with these data and the satellite-derived snow water equivalent.

After calibration of the different parameters, the four models show good performances of the components of the hydrological cycle compared to the real ones. An overview of the hydrological balance taking place in both basins has thus been obtained.

On one hand, after calibration and validation, the SWAT+ model of Lake Erken performed notably well regarding the examined statistics. We obtained better statistics results with the SWAT+ model than with SWAT12 model in this watershed. Although SWAT+ is a new tool and has not been as widely used compared to its predecessor (SWAT), our results demonstrated its validity and effectiveness. We conclude that the SWAT+ can be used effectively to create hydrological models in lake basins.

On the other hand, despite the scarcity of data and the high degree of anthropization of the study area for the Mar Menor models, it has still been possible to evaluate the different components of the Mar Menor water balance. Therefore, the initial focus on simulating watershed hydrology, could provide a strong basis for further development with a focus on nutrient and ecosystem dynamics. Such further the developed model could be used for scenario simulations and help to better understand how climate and watershed management affect the downstream aquatic ecosystem. Beyond the Mar Menor study, the methodological approach applied in the present study can also be useful for many other highly anthropized sites where observed data are scarce.

These hydrological models can play a key role as predictive tools to assist in the management of water resources, especially in the Mar Menor area. The next steps of our work will focus on improving these models with agricultural operations, and with the calibration of other components such as sediment and nutrients. This will result in more complete and realistic models, which will later be hybridized with lake models to obtain general and holistic models of the hydrology and ecology of the Mar Menor and Lake Erken basin.

APPENDIX I: Description of the SWAT and SWAT+ model

The Soil and Water Assessment Tool (SWAT) (Arnold *et al.*, 2012) is a software that allows the development of hydrological watershed models. This tool has been used globally for the last 20 years in many different scenarios, conditions and scales. Since its creation, SWAT has been implemented periodically to meet the needs of the scientific community, allowing increasingly flexible and reliable modeling. This was the case until the limit of the framework that allowed the SWAT model to continue to improve was reached, and new foundations for the model were needed. In 2017, a new SWAT model (SWAT+) was released, which was intended to be able to make models much more flexible, complex and realistic.

The main components of the SWAT model are hydrology, climate, nutrient cycling, sediment transport, crop development, agricultural management and pesticide dynamics. SWAT is a continuous simulation model operating on a daily time scale.

Water dynamics are represented by fluctuations in the hydrologic response units (HRUs) in both the SWAT and SWAT+ models. Each HRU is a unique combination of land-use, slope, soil, and management activities, which are connected by a geographic information system (GIS) interface. As a consequence, SWAT and SWAT+ are "semi-distributed" models, where it is considered that the same combination of land-use, slope, soil and management activities will cause the same hydrological response (Mohammed *et al.*, 2018). The main driver of the SWAT and SWAT+ models is the water balance. The following equation represent this concept in both models:

$$SW_t = SW_o + \sum (V_i - Q_i - E_i - P_i - QR_i) \times \Delta t$$

where SW_t and SW_o represent the final and initial soil water content (mm/day); V_i represents the precipitation (mm/day); Q_i represents the surface runoff (mm/day); E_i represents the evapotranspiration (mm/day); P_i represents the percolation (mm/day); QR_i represents the return flow (mm/day); and Δt represents the time interval (day). The i term refers to the index.

The spatial heterogeneity of a catchment is preserved through topography by dividing the catchment into multiple sub-catchments. These sub-basins are further subdivided into Hydrological Response Units (HRU) based on soil characteristics, land uses and slope mapping. These subdivisions allow the model to reflect differences in evapotranspiration for different crops and soils (Neitsch *et al.*, 2011).

The new SWAT+ improves the runoff routing capabilities while preserving the model's computational efficiency and ease of use. This new version of SWAT treats watershed elements -including aquifers, land-use units, HRUs, ponds, and reservoirs- as spatial objects. In comparison to the older SWAT, this feature improves the flexibility of the basin's configuration and discretisation (Bieger *et al.*, 2017).

Appendix I.I Description of the SWAT parameters.

A description of SWAT and SWAT+ parameters used for these studies is presented below:

- **CN2:** The SCS curve number is a function of the soil's permeability, land use and antecedent soil water conditions. Typical curve numbers for moisture condition II are listed in the following tables for various land covers and soil types. These values are appropriate for a 5% slope. The curve number may be updated in plant, tillage, and harvest/ kill operations. If CNOP is never defined for these operations, the value set for CN2 will be used throughout the simulation. If CNOP is defined for an operation, the value for CN2 is used until the time of the operation containing the first CNOP value. From that point on, the model only uses operation CNOP values to define the curve number for moisture condition II. Values for CN2 and CNOP should be entered for pervious conditions. In HRUs with urban areas, the model will adjust the curve number to reflect the impact of the impervious areas.
- **Alpha:** Baseflow alpha factor (1/days). The baseflow recession constant, α_{gw} , is a direct index of groundwater flow response to changes in recharge. Values vary from 0.1-0.3 for land with slow response to recharge to 0.9-1.0 for land with a rapid response. Although the baseflow recession constant may be calculated, the best estimates are obtained by analyzing measured streamflow during periods of no recharge in the watershed. It is common to find the baseflow days reported for a stream gage or watershed. This is the number of days for base flow recession to decline through one log cycle. When baseflow days are known, the alpha factor can be calculated:

Equation 6. Alpha factor.

$$\alpha_{gw} = \frac{1}{N} \times \ln \left[\frac{Q_{gw,N}}{Q_{gw,0}} \right] = \frac{1}{BFD} \times \ln[10] = \frac{2.3}{BFD}$$

where α_{gw} is the baseflow recession constant, and BFD is the number of baseflow days for the watershed.

- **Esco:** Soil evaporation compensation factor. This coefficient has been incorporated to allow the user to modify the depth distribution used to meet the soil evaporative demand to account for the effect of capillary action, crusting and cracks. ESCO must be between 0.01 and 1.0. As the value for ESCO is reduced, the model is able to extract more of the evaporative demand from lower levels.
- **Epc0:** Plant uptake compensation factor. The amount of water uptake that occurs on a given day is a function of the amount of water required by the plant for transpiration, E_t , and the amount of water available in the soil, SW. If upper layers in the soil profile do not contain enough water to meet the potential water uptake, users may allow lower layers to compensate. The plant uptake compensation factor can range from 0.01 to 1.00. As epc0 approaches 1.0, the model allows more of the water uptake demand to be met by lower layers in the soil. As epc0 approaches 0.0, the model allows less variation from the original depth distribution to take place.
- **Perco:** Percolation coefficient - adjusts soil moisture for percolation to occur (1.0 = fc)

- **Revap_co:** Groundwater "revap" coefficient. Water may move from the shallow aquifer into the overlying unsaturated zone. In periods when the material overlying the aquifer is dry, water in the capillary fringe that separates the saturated and unsaturated zones will evaporate and diffuse upward. As water is removed from the capillary fringe by evaporation, it is replaced by water from the underlying aquifer. Water may also be removed from the aquifer by deep-rooted plants which are able to uptake water directly from the aquifer. This process is significant in watersheds where the saturated zone is not very far below the surface or where deep-rooted plants are growing. Because the type of plant cover will affect the importance of revap in the water balance, the parameters governing revap can be varied by land use. As REVAP approaches 0, movement of water from the shallow aquifer to the root zone is restricted. As REVAP approaches 1, the rate of transfer from the shallow aquifer to the root zone approaches the rate of potential evapotranspiration. The value for REVAP should be between 0.02 and 0.20. This variable, along with REVAPMN, is the reason a different groundwater file is created for each HRU rather than each subbasin.
- **Awc:** Available water capacity of the soil layer (mm H₂O/mm soil). The plant available water, also referred to as the available water capacity, is calculated by subtracting the fraction of water present at permanent wilting point from that present at field capacity, $WPFCAWC = AWC - WP$ where AWC is the plant available water content, FC is the water content at field capacity, and WP is the water content at permanent wilting point. Available water capacity is estimated by determining the amount of water released between in situ field capacity (the soil water content at soil matric potential of -0.033 MPa) and the permanent wilting point (the soil water content at soil matric potential of -1.5 MPa).
- **Flo_min:** Minimum aquifer storage to allow return flow in meters.
- **Revap_min:** Threshold depth of water in the shallow aquifer for "revap" or percolation to the deep aquifer to occur (mm H₂O). Movement of water from the shallow aquifer to the unsaturated zone is allowed only if the volume of water in the shallow aquifer is equal to or greater than REVAPMN. This variable, along with GW_REVAP, is the reason a different groundwater file is created for each HRU rather than each subbasin.
- **Surlag:** Surface runoff lag coefficient. In large subbasins with a time of concentration greater than 1 day, only a portion of the surface runoff will reach the main channel on the day it is generated. SWAT incorporates a surface runoff storage feature to lag a portion of the surface runoff release to the main channel. SURLAG controls the fraction of the total available water that will be allowed to enter the reach on any one day. Note that for a given time of concentration, as surlag decreases in value more water is held in storage. The delay in release of surface runoff will smooth the streamflow hydrograph simulated in the reach.
- **K:** Saturated hydraulic conductivity (mm/hr). The saturated hydraulic conductivity, K_{sat} , relates soil water flow rate (flux density) to the hydraulic gradient and is a measure of the ease of water movement through the soil. K_{sat} is the reciprocal of the resistance of the soil matrix to water flow.
- **Snofall_tmp:** Snowfall temperature (°C). Mean air temperature at which precipitation is equally likely to be rain as snow/freezing rain. The snowfall temperature should be between -5 °C and 5 °C. A default recommended for this variable is snofall_tmp = 1.0. It is required in watersheds where snowfall is significant.

- **Snomelt_tmp:** Snow melt base temperature (°C). The snow pack will not melt until the snow pack temperature exceeds a threshold value. The snow melt base temperature should be between -5°C and 5°C . A default recommended for this variable is $\text{snomelt_tmp} = 0.50$. It is required in watersheds where snowfall is significant.
- **Snomelt_max:** Melt factor for snow on June 21 ($\text{mm H}_2\text{O}/^{\circ}\text{C} \cdot \text{day}$). If the watershed is in the Northern Hemisphere, snomelt_max will be the maximum melt factor. If the watershed is in the Southern Hemisphere, snomelt_max will be the minimum melt factor. If no value for snomelt_max is entered, the model will set $\text{snomelt_max} = 4.5$. It is required in watersheds where snowfall is significant.
- **Snomelt_min:** Melt factor for snow on December 21 ($\text{mm H}_2\text{O}/^{\circ}\text{C} \cdot \text{day}$). If the watershed is in the Northern Hemisphere, snomelt_min will be the minimum melt factor. If the watershed is in the Southern Hemisphere, snomelt_min will be the maximum melt factor. If no value for snomelt_min is entered, the model will set $\text{snomelt_min} = 4.5$. It is required in watersheds where snowfall is significant.

Snomelt_max and snomelt_min allow the rate of snow melt to vary through the year. The variables account for the impact of snow pack density on snow melt. In rural areas, the melt factor will vary from 1.4 to 6.9 $\text{mm H}_2\text{O}/\text{day} \cdot ^{\circ}\text{C}$. In urban areas, values will fall in the higher end of the range due to compression of the snow pack by vehicles, pedestrians, etc. Urban snow melt studies in Sweden reported melt factors ranging from 3.0 to 8.0 $\text{mm H}_2\text{O}/\text{day} \cdot ^{\circ}\text{C}$. Studies of snow melt on asphalt gave melt factors of 1.7 to 6.5 $\text{mm H}_2\text{O}/\text{day} \cdot ^{\circ}\text{C}$.

- **Snomelt_lag:** Snow pack temperature lag factor. The influence of the previous day's snow pack temperature on the current day's snow pack temperature is controlled by a lagging factor. The lagging factor inherently accounts for snow pack density, snow pack depth, exposure and other factors affecting snow pack temperature. Timp can vary between 0.01 and 1.0. As the lagging factor approaches 1.0, the mean air temperature on the current day exerts an increasingly greater influence on the snow pack temperature and the snow pack temperature from the previous day exerts less and less influence. As snomelt_lag goes to zero, the snow pack's temperature will be less influenced by the current day's air temperature. If no value for snomelt_lag is entered, the model will set $\text{snomelt_lag} = 1.0$. It is required in watersheds where snowfall is significant.
- **Sol_bd:** Moist bulk density (Mg/m^3 or g/cm^3). The soil bulk density expresses the ratio of the mass of solid particles to the total volume of the soil, $\rho_b = M_s / V_T$. In moist bulk density determinations, the mass of the soil is the oven dry weight and the total volume of the soil is determined when the soil is at or near field capacity. Bulk density values should fall between 1.1 and 1.9 Mg/m^3 .

- **Canmx:** Maximum canopy storage (mm H₂O). The plant canopy can significantly affect infiltration, surface runoff and evapotranspiration. As rain falls, canopy interception reduces the erosive energy of droplets and traps a portion of the rainfall within the canopy. The influence the canopy exerts on these processes is a function of the density of plant cover and the morphology of the plant species. When calculating surface runoff, the SCS curve number method lumps canopy interception in the term for initial abstractions. This variable also includes surface storage and infiltration prior to runoff and is estimated as 20% of the retention parameter value for a given day. When the Green and Ampt infiltration equation is used to calculate infiltration, the interception of rainfall by the canopy must be calculated separately. SWAT allows the maximum amount of water that can be held in canopy storage to vary from day to day as a function of the leaf area index. CANMX is the maximum amount of water that can be trapped in the canopy when the canopy is fully developed (mm H₂O).
- **Cherod:** Channel lte erodibility factor (0=non-erosive channel; 1=no resistance to erosion).
- **Cov:** Channel lte cover factor (0=channel is completely protected from erosion; 1=no vegetative cover on channel).
- **Usle_p:** USLE equation support practice factor. The support practice factor, PUSLE, is defined as the ratio of soil loss with a specific support practice to the corresponding loss with up-and-down slope culture. Support practices include contour tillage, stripcropping on the contour, and terrace systems. Stabilized waterways for the disposal of excess rainfall are a necessary part of each of these practices. Contour tillage and planting provides almost complete protection against erosion from storms of low to moderate intensity, but little or no protection against occasional severe storms that cause extensive breakovers of contoured rows. Contouring is most effective on slopes of 3 to 8 percent.
- **Usle_k:** USLE equation soil erodibility (K) factor (units: 0.013 (metric ton m² hr)/(m³-metric ton cm)). Some soils erode more easily than others even when all other factors are the same. This difference is termed soil erodibility and is caused by the properties of the soil itself. The soil erodibility factor is defined as the soil loss rate per erosion index unit for a specified soil as measured on a unit plot. A unit plot is 22.1-m (72.6-ft) long, with a uniform length-wise slope of 9-percent, in continuous fallow, tilled up and down the slope. Continuous fallow is defined as land that has been tilled and kept free of vegetation for more than 2 years. The units for the USLE soil erodibility factor in MUSLE are numerically equivalent to the traditional English units of 0.01 (ton acre hr)/(acre ft-ton inch). A soil type usually becomes less erodible with decrease in silt fraction, regardless of whether the corresponding increase is in the sand fraction or clay fraction.
- **Prf:** Peak rate adjustment factor for sediment routing in the main channel. Sediment routing is a function of peak flow rate and mean daily flow. Because SWAT originally could not directly calculate the sub-daily hydrograph, this variable was incorporated to allow adjustment

for the effect of the peak flow rate on sediment routing. These variable impacts channel degradation. If no value for PRF is entered, the model will set PRF = 1.0.

- **Cdn:** Denitrification exponential rate coefficient. This coefficient allows the user to control the rate of denitrification. Acceptable values for CDN range from 0.0 to 3.0. If no value for CDN is specified, the model will set CDN = 1.4.
- **Erorgn:** Organic N enrichment ratio for loading with sediment. As surface runoff flows over the soil surface, part of the water's energy is used to pick up and transport soil particles. The smaller particles weigh less and are more easily transported than coarser particles. When the particle size distribution of the transported sediment is compared to that of the soil surface layer, the sediment load to the main channel has a greater proportion of clay sized particles. In other words, the sediment load is enriched in clay particles. Organic nitrogen in the soil is attached primarily to colloidal (clay) particles, so the sediment load will also contain a greater proportion or concentration of organic N than that found in the soil surface layer. The enrichment ratio is defined as the ratio of the concentration of organic nitrogen transported with the sediment to the concentration in the soil surface layer. SWAT will calculate an enrichment ratio for each storm event, or allow the user to define a particular enrichment ratio for organic nitrogen that is used for all storms during the simulation. To calculate the enrichment ratio, the value for ERORGN is set to zero. The default option is to allow the model to calculate the enrichment ratio.
- **Nperco:** Nitrate percolation coefficient. NPERCO controls the amount of nitrate removed from the surface layer in runoff relative to the amount removed via percolation. The value of NPERCO can range from 0.01 to 1.0. As NPERCO \rightarrow 0.0, the concentration of nitrate in the runoff approaches 0. As NPERCO \rightarrow 1.0, surface runoff has the same concentration of nitrate as the percolate. If no value for NPERCO is entered, the model will set NPERCO = 0.20.
- **N_updis:** Nitrogen uptake distribution parameter. Root density is greatest near the surface, and plant nitrogen uptake in the upper portion of the soil will be greater than in the lower portion. The depth distribution of nitrogen uptake is controlled by β_n , the nitrogen uptake distribution parameter. The importance of the nitrogen uptake distribution parameter lies in its control over the maximum amount of nitrate removed from the upper layers. Because the top 10 mm of the soil profile interacts with surface runoff, the nitrogen uptake distribution parameter will influence the amount of nitrate available for transport in surface runoff. The model allows lower layers in the root zone to fully compensate for lack of nitrate in the upper layers, so there should not be significant changes in nitrogen stress with variation in the value used for β_n . If no value for N_UPDIS is entered, the model will set N_UPDIS = 20.0.
- **Sdcno:** Denitrification threshold water content. Fraction of field capacity water content above which denitrification takes place. Denitrification is the bacterial reduction of nitrate, NO_3^- , to N_2 or N_2O gases under anaerobic (reduced) conditions. Because SWAT does not track

the redox status of the soil layers, the presence of anaerobic conditions in a soil layer is defined by this variable. If the soil water content calculated as fraction of field capacity is \geq SDNCO, then anaerobic conditions are assumed to be present and denitrification is modeled. If the soil water content calculated as a fraction of field capacity is $<$ SDNCO, then aerobic conditions are assumed to be present and denitrification is not modeled. If no value for SDNCO is specified, the model will set SDNCO = 1.10.

- **Lat_orgn**: Organic nitrogen concentration in the base flow (mg/L) (range 0.0 – 200.0) default = 0.0.
- **Erorgp**: Phosphorus enrichment ratio for loading with sediment. The enrichment ratio is defined as the ratio of the concentration of phosphorus transported with the sediment to the concentration of phosphorus in the soil surface layer. SWAT will calculate an enrichment ratio for each storm event, or allow the user to define a particular enrichment ratio for phosphorus attached to sediment that is used for all storms during the simulation. If the value for ERORGP is set to zero, the model will calculate an enrichment ratio for every storm event. The default option is to allow the model to calculate the enrichment ratio.
- **Phoskd**: Phosphorus soil partitioning coefficient (m^3/Mg). The phosphorus soil partitioning coefficient is the ratio of the soluble phosphorus concentration in the surface 10 mm of soil to the concentration of soluble phosphorus in surface runoff. The primary mechanism of phosphorus movement in the soil is by diffusion. Diffusion is the migration of ions over small distances (1-2 mm) in the soil solution in response to a concentration gradient. Due to the low mobility of solution phosphorus, surface runoff will only partially interact with the solution P stored in the top 10 mm of soil. If no value for PHOSKD is entered, the model will set PHOSKD = 175.0.
- **Psp**: Phosphorus availability index. Many studies have shown that after an application of soluble P fertilizer, solution P concentration decreases rapidly with time due to reaction with the soil. This initial “fast” reaction is followed by a much slower decrease in solution P that may continue for several years. In order to account for the initial rapid decrease in solution P, SWAT assumes a rapid equilibrium exists between solution P and an “active” mineral pool. The subsequent slow reaction is simulated by the slow equilibrium assumed to exist between the “active” and “stable” mineral pools. Equilibration between the solution and active mineral pool is governed by the phosphorus availability index. This index specifies the fraction of fertilizer P which is in solution after an incubation period, i.e. after the rapid reaction period. A number of methods have been developed to measure the phosphorus availability index. The one used in SWAT uses various amounts of phosphorus are added in solution to the soil as K_2HPO_4 . The soil is wetted to field capacity and then dried slowly at 25°C . When dry, the soil is rewetted with deionized water. The soil is exposed to several wetting and drying cycles over a 6-month incubation period. At the end of the incubation period, solution

phosphorus is determined by extraction with anion exchange resin. The P availability index is then calculated:

$$pai = \frac{P_{solution,f} - P_{solution,i}}{fert_{minP}}$$

where pai is the phosphorus availability index, $P_{solution,f}$ is the amount of phosphorus in solution after fertilization and incubation, $P_{solution,i}$ is the amount of phosphorus in solution before fertilization, and $fert_{minP}$ is the amount of soluble P fertilizer added to the sample. If no value for PSP is entered, the model will set PSP = 0.40.

- **P_updis:** Phosphorus uptake distribution parameter. This parameter controls plant uptake of phosphorus from the different soil horizons in the same way that UBN controls nitrogen uptake. Phosphorus removed from the soil by plants is taken from the solution phosphorus pool. The importance of the phosphorus uptake distribution parameter lies in its control over the maximum amount of solution P removed from the upper layers. Because the top 10 mm of the soil profile interacts with surface runoff, the phosphorus uptake distribution parameter will influence the amount of labile phosphorus available for transport in surface runoff. The model allows lower layers in the root zone to fully compensate for lack of solution P in the upper layers, so there should not be significant changes in phosphorus stress with variation in the value used for β_p . If no value for P_UPDIS is entered, the model will set P_UPDIS = 20.0.
- **Lat_orgp:** Organic phosphorus concentration in the base flow (mg/L) (range 0.0 – 200.0) default = 0.0.

APPENDIX II: Bibliography

- Abbaspour, K. C. (2013). Swat-cup 2012. *SWAT calibration and uncertainty program—A user manual*.
- Adam, J. C., Hamlet, A. F., & Lettenmaier, D. P. (2009). Implications of global climate change for snowmelt hydrology in the twenty-first century. *Hydrological Processes: An International Journal*, 23(7), 962-972.
- Aguilar Escribano, J., Gimenez-Casalduero, F., Mas Hernández, J., & Ramos-Esplá, A. A. (2016). Evaluación del estado y composición de la Comunidad Fitoplanctónica de las agua del Mar Menor, Murcia (mayo de 2016).
- Arino, O., Ramos, J., Kalogirou, V., Defourny, P. & Achard, F. (2010). Globcover 2009. In *Proceedings of ESA Living Planet Symposium*, Bergen, Norway, 28 June–2 July, pp. 686–689.
- Arnold, J. G., Moriasi, D. N., Gassman, P. W., Abbaspour, K. C., White, M. J., Srinivasan, R., Santhi, C., Harmel, R. D., van Griensven, A., Van Liew, M. W., Kannan, N., & Jha, M. K. (2012). SWAT: Model use, calibration, and validation. *Transactions of the ASABE*, 55(4), 1491-1508.
- Bieger, K.; Arnold, J.G.; Rathjens, H.; White, M.J.; Bosch, D.D.; Allen, P.M.; Volk, M.; Srinivasan, R. (2017). Introduction to SWAT+, a completely restructured version of the soil and water assessment tool. *JAWRA Journal of the American Water Resources Association*, 53(1), 115-130.
- Brekke, L. D., Miller, N. L., Bashford, K. E., Quinn, N. W., & Dracup, J. A. (2004). Climate change impacts uncertainty for water resources in the san joaquin river basin, california 1. *JAWRA Journal of the American Water Resources Association*, 40(1), 149-164.
- Chawanda, C. J. (2021). SWAT+ Toolbox: User Manual; SWAT+, Soil & Water Assesment Tool. Available online: <https://www.openwater.network/assets/downloads/SWATplusToolbox-UserMannual.pdf>. (Accessed on 1 December 2021).
- Cibir, R., Sudheer, K. P., & Chaubey, I. (2010). Sensitivity and identifiability of stream flow generation parameters of the SWAT model. *Hydrological Processes: An International Journal*, 24(9), 1133-1148.
- Esteve Selma, M.A.; Martínez Martínez, J.; Fitz, C.; Robledano F.; Martínez Paz, J.M.; Carreño, M.F.; Guaita, N.; Martínez López, J. & Miñano, J. (2016). Conflictos ambientales derivados de la intensificación de los usos en la cuenca del Mar Menor: una aproximación interdisciplinar. En Víctor M. León and Jose M^a Bellido (Eds). *Mar Menor: una laguna singular y sensible. Evaluación científica de su estado*. Madrid, Instituto Español de Oceanografía, Ministerio de Economía y Competitividad. *Temas de Oceanografía*, 9, 79-112.
- Farr, T. G., & Kobrick, M. (2000). Shuttle Radar Topography Mission produces a wealth of data. *Eos, Transactions American Geophysical Union*, 81(48), 583-585.
- Gassman, P. W., Reyes, M. R., Green, C. H., & Arnold, J. G. (2007). The soil and water assessment tool: historical development, applications, and future research directions. *Transactions of the ASABE*, 50(4), 1211-1250.
- Grusson, Y., Sun, X., Gascoin, S., Sauvage, S., Raghavan, S., Anctil, F., & Sánchez-Pérez, J. M. (2015). Assessing the capability of the SWAT model to simulate snow, snow melt and stream-flow dynamics over an alpine watershed. *Journal of Hydrology*, 531, 574-588

- Gupta, H. V., Sorooshian, S., & Yapo, P. O. (1999). Status of automatic calibration for hydrologic models: Comparison with multilevel expert calibration. *Journal of Hydrologic Engineering*, 4(2), 135-143.
- Gupta, H. V., Kling, H., Yilmaz, K. K., & Martinez, G. F. (2009). Decomposition of the mean squared error and NSE performance criteria: Implications for improving hydrological modeling. *Journal of hydrology*, 377(1-2), 80-91.
- Ha, L. T., Bastiaanssen, W. G., Van Griensven, A., Van Dijk, A. I., & Senay, G. B. (2018). Calibration of spatially distributed hydrological processes and model parameters in SWAT using remote sensing data and an auto-calibration procedure: A case study in a Vietnamese river basin. *Water*, 10(2), 212.
- Hargreaves, G. H. (1994). Defining and using reference evapotranspiration. *Journal of irrigation and drainage engineering*, 120(6), 1132-1139.
- Jiménez-Martínez, J., García-Aróstegui, J. L., Hunink, J. E., Contreras, S., Baudron, P., & Candela, L. (2016). The role of groundwater in highly human-modified hydrosystems: a review of impacts and mitigation options in the Campo de Cartagena-Mar Menor coastal plain (SE Spain). *Environmental Reviews*, 24(4), 377-392.
- Jiménez-Navarro, I. C. (2020). Tanatocenosis malacológica como registro de los procesos ecológicos del Mar Menor en las últimas décadas. In *Tendencias medioambientales en el ámbito universitario: I Congreso nacional de TFG Y TFM ambientales" Tendencias medioambientales en el ámbito universitario"*, Burgos 7-9 noviembre 2019 (pp. 622-645). Universidad de Burgos.
- Jiménez-Navarro, I. C., Jimeno-Sáez, P., López-Ballesteros, A., Pérez-Sánchez, J., & Senent-Aparicio, J. (2021). Impact of Climate Change on the Hydrology of the Forested Watershed That Drains to Lake Erken in Sweden: An Analysis Using SWAT+ and CMIP6 Scenarios. *Forests*, 12(12), 1803.
- Kouchi, D. H., Esmaili, K., Faridhosseini, A., Sanaeinejad, S. H., Khalili, D., & Abbaspour, K. C. (2017). Sensitivity of calibrated parameters and water resource estimates on different objective functions and optimization algorithms. *Water*, 9(6), 384.
- Le Moal, M., Gascuel-Oudou, C., Ménesguen, A., Souchon, Y., Étrillard, C., Levain, A., Moatar, F., Pannard, A., Souchu, P., Lefebvre, A. & Pinay, G. (2019). Eutrophication: a new wine in an old bottle?. *Science of the Total Environment*, 651, 1-11.
- Loujus, K., Pulliainen, J., Takala, M., Moisander, M., Cohen, J., Ikonen, J. & Lemmetyinen, J. (2017). Copernicus Global Land Operations “Cryosphere and Water” Preliminary Quality Assessment Report, SnowWater Equivalent. In *Copernicus Global Land Operations*; European Commission Joint Research Centre: Sevilla, Spain.
- Malagò, A., Pagliero, L., Bouraoui, F., & Franchini, M. (2015). Comparing calibrated parameter sets of the SWAT model for the Scandinavian and Iberian peninsulas. *Hydrological Sciences Journal*, 60(5), 949-967.
- Malmaeus, J. M., & Håkanson, L. (2004). Development of a lake eutrophication model. *Ecological Modelling*, 171(1-2), 35-63.
- Martens, B., Miralles, D. G., Lievens, H., Van Der Schalie, R., De Jeu, R. A., Fernández-Prieto, D., Beck, H. E., Doringo, W. A. & Verhoest, N. E. C. (2017). GLEAM v3: Satellite-based land

- evaporation and root-zone soil moisture. *Geoscientific Model Development*, 10(5), 1903-1925.
- Miralles, D. G., Holmes, T. R. H., De Jeu, R. A. M., Gash, J. H., Meesters, A. G. C. A., & Dolman, A. J. (2011). Global land-surface evaporation estimated from satellite-based observations. *Hydrology and Earth System Sciences*, 15(2), 453-469.
 - Mohammed, I. N., Bolten, J. D., Srinivasan, R., & Lakshmi, V. (2018). Improved hydrological decision support system for the Lower Mekong River Basin using satellite-based earth observations. *Remote sensing*, 10(6), 885.
 - Molina-Navarro, E., Martínez-Pérez, S., Sastre-Merlín, A., & Bienes-Allas, R. (2014). Hydrologic modeling in a small Mediterranean basin as a tool to assess the feasibility of a limno-reservoir. *Journal of environmental quality*, 43(1), 121-131.
 - Morales Yago, F. J. (2013). El impacto de la actividad turística sobre el paisaje de La Manga del Mar Menor (Murcia). *Estudios geográficos*, 74(275), 523-556.
 - Moriasi, D. N., Arnold, J. G., Van Liew, M. W., Bingner, R. L., Harmel, R. D. & Veith, T. L. (2007). Model evaluation guidelines for systematic quantification of accuracy in watershed simulations. *Transactions of the ASABE*, 50(3), 885-900.
 - Moriasi, D. N., Gitau, M. W., Pai, N., & Daggupati, P. (2015). Hydrologic and water quality models: Performance measures and evaluation criteria. *Transactions of the ASABE*, 58(6), 1763-1785.
 - Nachtergaele, F., van Velthuizen, H., Verelst, L., Batjes, N. H., Dijkshoorn, K., van Engelen, V. W. P., Fischer, G., Jones, A., & Montanarella, L. (2010). The Harmonized World Soil Database. In R. J. Gilkes, & N. Prakongkep (Eds.), *Proceedings of the 19th World Congress of Soil Science, Soil Solutions for a Changing World, Brisbane, Australia, 1-6 August 2010* (pp. 34-37). International Union of Soil Sciences. <https://edepot.wur.nl/154132>
 - Nash, J. E.; Sutcliffe, J. (1970). River flow forecasting through conceptual models' part I - A discussion of principles. *Journal of Hydrology*, 10(3), 282-290.
 - Nash, J. E., & Sutcliffe, J. V. (1970). River flow forecasting through conceptual models' part I—A discussion of principles. *Journal of hydrology*, 10(3), 282-290.
 - Neitsch, S. L., Arnold, J. G., Kiniry, J. R., & Williams, J. R. (2011). Soil and water assessment tool theoretical documentation version 2009. *Texas Water Resources Institute*.
 - Oudin, L., Hervieu, F., Michel, C., Perrin, C., Andréassian, V., Anctil, F., & Loumagne, C. (2005). Which potential evapotranspiration input for a lumped rainfall–runoff model?: Part 2—Towards a simple and efficient potential evapotranspiration model for rainfall–runoff modeling. *Journal of hydrology*, 303(1-4), 290-306.
 - Odusanya, A. E., Mehdi, B., Schürz, C., Oke, A. O., Awokola, O. S., Awomeso, J. A., Adejuwon, J. O. & Schulz, K. (2019). Multi-site calibration and validation of SWAT with satellite-based evapotranspiration in a data-sparse catchment in southwestern Nigeria. *Hydrology and Earth System Sciences*, 23(2), 1113-1144.

- Paul, P. R., Rao, L. V. R., & Sankar, E. S. (1994). Estimation of basin snow water equivalent (SWE) using accumulation and depletion patterns of snowcover from optical satellite data. *GIS Development*.
- Pradhanang, S. M., Anandhi, A., Mukundan, R., Zion, M. S., Pierson, D. C., Schneiderman, E. M., Matonse, A. & Frei, A. (2011). Application of SWAT model to assess snowpack development and streamflow in the Cannonsville watershed, New York, USA. *Hydrological Processes*, 25(21), 3268-3277.
- Puertes, C., Bautista, I., Lidón, A., & Francés, F. (2021). Best management practices scenario analysis to reduce agricultural nitrogen loads and sediment yield to the semiarid Mar Menor coastal lagoon (Spain). *Agricultural Systems*, 188, 103029.
- Senent-Aparicio, J., Pérez-Sánchez, J., García-Aróstegui, J. L., Bielsa-Artero, A., & Domingo-Pinillos, J. C. (2015). Evaluating groundwater management sustainability under limited data availability in semiarid zones. *Water*, 7(8), 4305-4322.
- Sobol, I. M. (2001). Global sensitivity indices for nonlinear mathematical models and their Monte Carlo estimates. *Mathematics and computers in simulation*, 55(1-3), 271-280.
- Sun, C., & Ren, L. (2013). Assessment of surface water resources and evapotranspiration in the Haihe River basin of China using SWAT model. *Hydrological processes*, 27(8), 1200-1222.
- Tarboton, D. G., Chowdhury, T. G., & Jackson, T. H. (1994). A spatially distributed energy balance snowmelt model.
- Tobin, K. J., & Bennett, M. E. (2017). Constraining SWAT calibration with remotely sensed evapotranspiration data. *JAWRA Journal of the American Water Resources Association*, 53(3), 593-604.
- Velasco, J., Lloret, J., Millán, A., Marin, A., Barahona, J., Abellán, P., & Sánchez-Fernández, D. (2006). Nutrient and particulate inputs into the Mar Menor lagoon (SE Spain) from an intensive agricultural watershed. *Water, Air, and Soil Pollution*, 176(1), 37-56.
- Velasco, A. M., Pérez-Ruzafa, A., Martínez-Paz, J. M., & Marcos, C. (2018). Ecosystem services and main environmental risks in a coastal lagoon (Mar Menor, Murcia, SE Spain): The public perception. *Journal for Nature Conservation*, 43, 180-189.
- Zeinivand, H., & De Smedt, F. (2009). Hydrological modeling of snow accumulation and melting on river basin scale. *Water resources management*, 23(11), 2271-2287.



SMARTLAGOON

End of Deliverable 3.1



This project has received funding from the European Union's Horizon 2020 research and innovation programme under grant agreement No 101017861.